TRANSNUCLEAR

CALCULATION PACKAGE

CALCULATION NO:	NUH 24PTH.0421	PROJECT NAME:	NUHOMS® 24PTH Design
PROJECT NO:	NUH 24PTH	CLIENT:	Transnuclear, Inc.

CALCULATION TITLE:

Thermal Analysis of the HSM-H Loaded with a NUHOMS®- 24PTH DSC - Storage Conditions.

SUMMARY DESCRIPTION:

This calculation determines the temperature distribution in the HSM-H loaded with a 24PTH DSC for normal, off-normal, and accident conditions.

This calculation was prepared under TN Hawthorne QA procedures (Calculation No. 60977-3). TN-Fremont has reviewed this calculation and accepted it for use in the NUHOMS®-24PTH project with the following comments/clarifications:

1) The revision of Ref. 1 is Rev. 0
2) The ref. 2 drawing numbers (HSM-H-01 to HSM-H-06) have been renumbered as NUH-03-7001 sheets 1 to 10, Rev. 0). Any differences between the HSM-H-01 to –06 sketches and the NUH-03-7001 drawings have been addressed in the calculation.
3) The correct ref. 3 calc. Number is 60977-2, not 10494-26.

NON-PROPRIETARY
FOR INFORMATION ONLY

REVISION	TOTAL PAGES AND DISKS (IF ANY)	NAMES AND INITIALS OF PREPARERS & DATES	NAMES AND INITIALS OF VERIFIERS & DATES	APPROVER NAME AND SIGNATURE	APPROVAL DATE
0	61 (2 cover sheets+59 main body) 1CD*	N/A	N/A	Miguel M. Manrique Miguel A. Manrique	9/18/03

* Proprietary Information - Intentionally Left Out

TRANSNUCLEAR

Form 3.1-1
Calculation Approval Sheet

Project Name: NUHOMS-24PT H **Project #:** 60977

Calculation Title: Thermal Analysis of the HSM-H Storage Conditions

Calculation #: 60977-3 **Draft/Revision #:** 0 **DCR #:** ---

Number of pages: 59

Number of CDs attached: 1

If original issue, 10CFR72.48 review required?
[X] No (explain) **[ ] Yes, SR No.** ____________
This calculation is performed to support amendment application

1. **This calculation is complete and ready for independent review**

   Originator's Signature ____________ Date: 9/4/03

2. **This calculation has been checked for consistency, completeness, and arithmetic correctness.**

   Checker Signature ____________ Date: 9/4/03

3. **Calculation preparation and check complies with procedure - package is complete**

   PE's Signature ____________ Date: 9/4/03

1 – Objective

Determine the temperature distribution in the HSM of NUHOMS-24PTH system for normal, off-normal and accident storage conditions.

2 – References

1. "Design Criteria for the NUHOMS-24PTHsystem for Transport and storage" - Specification # NUH24PTH.0101
2. NUHOMS HSM Model H, Drawings HSM-H-01 to HSM-H-06, revision 0 and NUHOMS-24PTH DSC Drawing, NUH24PTH -1001, rev. 0
3. Calculation 10494-26, rev. 0, "Air Flow Calculation for NUHOMS-24PTH"
4. NRC, Code of Federal Regulations, Part 71, "Packaging and Transportation of Radioactive Material", 2003
5. Siegel, Howell, "Thermal Radiation Heat Transfer", 4th Edition, 2002
6. ASME Boiler and Pressure Vessel Code, Section II, Part D, "Material Properties", 1998 and 2000 addenda
7. Zoldners, "Thermal Properties of Concrete under Sustained Elevated Temperatures", ACI Publications, Paper SP 25-1, American Concrete Institute, Detroit, MI, 1970
8. Project 10982, Specification # E-19836, rev. 0, "Precast Concrete Construction of NUHOMS HSM"
9. Cavanaugh, "Guide to Thermal Properties of Concrete and Masonary Systems", Reported by ACI Committee 122, Report # ACI 122R-02, American Concrete Institute, Detroit, MI, 2002
10. Test Report, Azzazy Technology, Inc., "Emissivity Measurements of 304 Stainless Steel", Report No. ATI-2000-09-601, 2000
11. Bentz, "A Computer Model to Predict the Surface Temperature and Time-of-wetness of Concrete Pavements and Bridge Decks", Report # NISTIR 6551, National Institute of Standards and Technology, 2000
12. Kreith, "Principles of Heat Transfer", 3rd Edition, 1973
13. Perry, Hilton, "Chemical Engineers' Handbook", 5th Edition, 1973
14. Rohsenow, Hartnett, "Handbook of Heat Transfer Fundamentals", 2nd Edition, 1985
15. Kreith, "The CRC Handbook of Thermal Engineering", 2000
16. ASHRAE Handbook Fundamentals, 4th Edition, 1983
17. Calculation NUH-04.0421, Rev. 6, "Qualification of Paint on Heat Shield for a Standardized NUHOMS HSM Design", Project No. NUH-04
18. Calculation NUH24PTH.0450, Rev. 0, "Thermal Evaluation of the NUHOMS OS197H Transfer Cask"

19. Calculation NUH24PTH.0403, Rev. 0, " NUHOMS-24PTH-DSC Thermal Evaluation for Storage and Transfer Conditions"
20. ANSYS Computer Code and User's Manuals, Rev. 6.0. See Test Report E-19197, Rev. 0 and E-20184, Rev. 0 for validation of computer code.
21. ANSYS files: / Calc60977-3 / HSMH_24s.db, HSMH_24s.sub, hsmh24.rth, hsmh24c.rth, hsmh32.rth, hsmh32c.rth, hsmh32w.rth, hsmh41h.rth, hsmh41.rth, hsmh41c0.rth, hsmh41c40.rth, hsmh41h1.rth, hsme_24s.db, hsme_24s.rth hsme_24s.sub HC_ROOF.mac, HC_FRONT.mac, HC_VPL.mac, HC_HCL.mac, HC_HPLU.mac, HC_HPLD.mac, HC_IPLU.mac, HC_IPLD.mac, HC_Louver.mac, HCIPLUm.mac Calc60997-3.xls

3 – Discussion and Assumptions

Horizontal Storage Module, type H (HSM-H) is designed to provide an independent, passive system with substantial structural capacity to ensure safe storage of spent fuel assemblies in NUHOMS-24PTH canisters. The decay heat load from stored canisters is removed via combination of radiation, convection and conduction. Ambient air enters the HSM through ventilation inlet openings in the lower part of the HSM side walls and circulates around the DSC and the side heat shields. Warm air passes through the top heat shield and exits the HSM through the outlet openings in the upper part of the HSM side walls.

Decay heat is rejected from the DSC to the HSM air space by convection and then is removed from the HSM by natural air circulation. Heat is also radiated from the DSC surface to the heat shields and HSM walls, where natural air circulation and conduction through the walls remove the heat. Typical flow paths are shown in Figure 1.

This analysis determines the temperature distribution on the DSC shell, which is used to calculate the fuel peak cladding temperature in a detailed model of the DSC. The HSM wall temperatures are also determined in this analysis.

Three maximum decay heat loads are considered for the NUHOMS-24PTH system. The maximum decay heat loads are: 24kW, 31.2 kW, and 40.8 kW.

Ambient temperatures between 0-100°F are considered as normal storage conditions and maximum day temperature of 117°F is considered as off-normal, hot storage condition [1]. The lowest ambient temperature is considered to be -40°F [1].

Since the HSM-H is located outdoors, there is a remote probability that the air inlet and outlet openings become blocked by debris from events such as flooding, high wind, and tornados. The perimeter security fence around ISFSI and the location of the air inlet and outlet openings reduces the probability of such an accident. Nevertheless, complete blockage of the inlet and outlet vents are considered conservatively as an accident case in this analysis.

The thermal mass of the HSM, the construction of the HSM ventilation system, and the location of the fuel on the transfer vehicle limit the effect of a fire accident for the HSMs. The worst case fire accident is commonly bounded by the fire accident case during transfer operation. Therefore, this analysis considers the blocked vent accident case as the only accident case with relevant thermal effects.

The temperature responses of the HSM and DSC to maximum day temperature are relatively slow because of their large thermal inertia. Therefore, considering an average maximum temperature over a 24 hour period is reasonable to calculate the maximum component temperatures for the HSM and DSC using steady state boundary conditions.

In order to calculate a daily average temperature given a maximum day temperature, a minimum daily range must be specified. From Table 1 in chapter 24 of reference [16], the minimum mean daily range in the contiguous United States is 27°F for a maximum summer ambient above 110°F. The method of calculating the daily average temperature is described in chapter 26.6 of reference [16]. In this method the hourly temperature is defined as:

$T_{hour} = T_{max}$ – (percentage of the daily range) x (mean daily range)

The percentages of the daily range are shown as a function of day time in Table 3, chapter 26 of [16]. The average of the hourly temperatures over the 24 hour period gives the daily average temperature. Table 1 shows the calculated daily average temperature for a maximum day temperature of 117°F and a minimum daily range of 27°F.

Table 1 – Daily Average Temperature

Maximum day temperature = 117°F
Minimum daily range = 27°F

Time, hr	% daily range [16]	T_{hour} (°F)		Time, hr	% daily range 16]	T_{hour} (°F)
1	87	93.5		13	11	114.0
2	92	92.2		14	3	116.2
3	96	91.1		15	0	117.0
4	99	90.3		16	3	116.2
5	100	90.0		17	10	114.3
6	98	90.5		18	21	111.3
7	93	91.9		19	34	107.8
8	84	94.3		20	47	104.3
9	71	97.8		21	58	101.3
10	56	101.9		22	68	98.6
11	39	106.5		23	76	96.5
12	23	110.8		24	82	94.9

Daily average temperature = 102°F

An ambient temperature of 105°F is used in this analysis to bound the maximum temperatures for normal and off-normal storage conditions.

To maximize the temperature gradients in the HSM concrete structure, ambient temperature of -40°F is considered for the off-normal cold storage condition. To consider the maximum thermal stresses in structural evaluation, the temperature distribution in the HSM is also calculated at 0 and 100°F ambient temperatures for the maximum decay heat load of 40.8 kW.

The temperature distributions for the normal and off-normal conditions are determined using steady-state models. For accident case, a transient model is developed, which has a coarser mesh than the steady-state model to avoid problems with the computational resources.

For the steady-state runs, a half symmetric, three dimensional, finite element model of the HSM-H is developed using ANSYS [20] to determine the maximum temperatures for the normal and off-normal conditions. Conduction through components is modeled using SOILD70 elements. Radiation between the DSC shell, heat shields, and HSM walls is modeled using /AUX12 methodology. SHELL57 elements were superimposed on radiating surfaces to create the super-element MATRIX50. These SHELL57 elements were unselected prior to solving the model. To reduce the number of nodes in the super-element, the web of the supporting beam is modeled using SHELL57 elements. Radiation is therefore not applied on the web of the supporting beam. This assumption is valid, since the web is mainly covered from the DSC radiation by the flanges of the supporting beam. Thickness of the web (0.55") is given as real constant to the SHELL57 elements representing the web.

The side shields are modeled as flat plates with a thickness of 0.3125" at the position of shield base plate. Convection from the fins attached to the side shields is modeled using equivalent convection coefficient. Calculation of the effective convection coefficients is discussed in Appendix A. Purpose of adding fins on the side heat shield is to provide more surface area for the convection. The excess surface area may not be required for decay heat loads lower than 40.8 kW. To show the effect of removing the fins, a DSC with decay heat load of 31.2 kW is considered in the HSM-H model without the fins on the side heat shield. In this case, the convection coefficient for a flat, vertical plate replaces the effective convection coefficient over the fins.

It is considered in this analysis that the side heat shield is fabricated completely out of Al-1100. Since the main purpose of the side heat shield is to protect the concrete walls against direct thermal radiation from the DSC, reducing the side heat shield conductivity from Al-1100 to stainless steel does not have any significant effect on the temperature distribution within the HSM, provided that the emissivity values of the front and back side of the heat shield remain unchanged.

The top shield is in the form of a louver hanging from the ceiling. The louver is also modeled as a flat plate with effective convection coefficients discussed in Appendix B.

The dimensions of the model are taken from [2]. The lower part of the HSM sidewall is offset by 6" toward the HSM cavity. The thickness of the offset wall is 18". To simplify the model, the HSM sidewall is considered as a straight, 12" thick wall without offsets. The effect of the offset on temperature distribution is evaluated in Appendix C. The steady-state finite element model is shown in Figures 2 to 5.

The circumference of the DSC model is divided into eight regions. The first region covers the area between the supporting rails from -90 to -64.2 degree angle. The second region begins from the center line of the supporting beam at -60 degree angle to -45 degree angle. The surface of the DSC shell from -64.4 to -60 degree angle is located above the upper edge of the slots in the slotted bar. The free convection is therefore restricted over this area. For conservatism, this area is considered as a dead zone with no free convection. The other circumferential regions are equal in size and each covers 22.5 degrees of the DSC shell. Figure 6 shows the regions of the DSC lower half. The bulk temperatures for the circumferential regions around the DSC are calculated in [3] and listed in Table 2.

The correlation for free convection over a horizontal cylinder is considered to calculate the convection coefficients for the circumferential DSC regions. Convection on HSM-H end walls is calculated using free convection correlations over vertical surfaces at HSM bulk air temperature. Air bulk temperature, T_s, is taken from [3].

Table 2 – Air Temperatures in the HSM Cavity*

	Max. Decay Heat	24 kW		31.2 kW		40.8 kW			
Location	Temperature	Amb. -40°F	Amb. 117°F	Amb. -40°F	Amb. 117°F	Amb. -40°F	Amb. 0°F	Amb. 100°F	Amb. 117°F
Lower part of HSM	T_0	-38	108	-37	109	-36	4	105	110
DSC Region 1	T_1	-35	112	-34	113	-33	8	110	115
DSC Region 2	T_2	-30	118	-28	121	-26	16	119	124
DSC Region 3	T_3	-25	125	-22	129	-19	23	129	134
DSC Region 4	T_4	-21	132	-17	137	-12	31	138	144
DSC Region 5	T_5	-16	138	-11	145	-5	39	148	153
DSC Region 6	T_6	-11	145	-5	153	2	47	158	163
DSC Region 7	T_7	-6	152	1	161	9	54	167	173
DSC Region 8	T_8	-1	159	7	169	16	62	177	182
Air Bulk Temp	T_s	-23	129	-19	134	-15	28	134	140

* The temperatures reported in Table 2 are maximum 3°F lower than the corresponding values calculated in the finalized version of [3]. The effect of this discrepancy is minimal on the maximum component temperatures in the HSM-H. See Appendix C for evidence.

Convection on the lower part of the side wall, below the side heat shield is determined using the free convection correlation over vertical surfaces at the cold region temperature (T_0). For the space between the side wall and the side shield, the free convection correlation for a narrow channel is used to determine the free convection coefficient.

For the HSM-H ceiling and the HSM-H basemat, correlations for flat horizontal surfaces are used to determine free convection coefficients. Air temperatures for the convection on the basemat and ceiling are T_1 and T_8 respectively. The calculation methods of free convection coefficients are discussed in detail in Appendix B. Figures 8 shows the convection boundary conditions applied in the model.

Insolance is considered on the roof and front wall of the HSM, which are exposed to the ambient. The values of the solar heat flux are taken from [4] averaged over a 24 hour period [1]. The insolance is applied as a constant heat flux over the SURF152 elements superimposed on the SOLID70 elements on the HSM roof and front wall. The absorptivity of the concrete surface is 0.73 - 0.91 at 300K [5]. For conservatism a solar absorptivity of 1 is considered for the exterior concrete surfaces. The values of the applied heat fluxes are listed below:

Shape	Insolance [4] (gcal/cm^2)	Averaged over 24 hr (Btu/hr-in^2)
HSM roof	800	0.8537
HSM front wall	200	0.2134

Insolance is not considered for the minimum ambient temperatures of 0 and -40°F.

Convection and radiation from the roof and the front wall are combined together as a total convection coefficient. The calculation of the total convection coefficient is discussed in Appendix B.

Since the HSM's are located side by side, the worst case for the maximum temperatures occurs when DSC's with the maximum decay heat load are stored in adjacent HSM's. To evaluate the worst case, adiabatic boundary conditions are applied over the outer surfaces of the HSM side walls and back wall.

The maximum temperature gradient occurs in a single or an end HSM, when one or two of the side walls are exposed to the cold ambient temperature. To bound the maximum temperature gradient across the HSM concrete walls, the HSM-H finite element model is modified, so that three foot shield walls are added to the side walls and the back wall of the HSM-H. An average gap of 0.125" is considered between the shield walls and the HSM-H module as defined in [2]. The modified model simulates a single HSM-H module

exposed to -40F ambient temperature without solar heat flux. The finite element model of the single HSM-H module is shown in Figure 7.

The DSC contents (fuel assemblies, basket, etc.) are not modeled for the steady state runs of normal and off-normal conditions. The decay heat load is considered to be distributed evenly on the radial inner surface of the DSC without using the peaking factors. This assumption is valid since the high conductivity of the basket plates and rails flattens the axial decay heat profile. The applied decay heat flux is:

$$Decay\ heat\ flux = \frac{Q}{\pi D_i L} \quad \text{Btu/hr-in}^2$$

where,
Q = decay heat load (24, 31.2, or 40.8 kW)
Di = inner DSC diameter = 66.19" [2]
L = DSC cavity length = 169.6" [2]

To maximize the applied heat flux, the minimum cavity length of DSC is used for L in the above equation.

It is assumed that soil has a temperature of 70°F at 10' below the HSM-H basemat for hot conditions. The soil temperature for cold condition (0°F or -40°F) is assumed to be 45°F. These assumptions are consistent with the assumptions in the thermal analysis of the standardized HSM design [17]. The HSM basemat is considered to be a 4' thick concrete slab. Due to low conductivity of concrete and soil, the model is insensitive to the thickness of the basemat / soil and the soil temperature. The boundary conditions applied in the model are shown in Figures 8 and 9.

To determine the maximum temperatures of the HSM and the DSC shell for the blocked vent accident case, the finite element model of the HSM-H is modified to a transient model. Elements with thermal properties of air are added in the finite element model to consider the convection in the closed HSM-H cavity during blockage of the vents. The mesh size of the model is slightly increased to avoid computer resource problems for the transient run.

The basket and the fuel assemblies for the transient case are modeled as a homogenized material with effective properties. Heat generating boundary conditions are applied uniformly on all elements representing the DSC content. The amount of generated heat per unit volume of the DSC content is calculated as follows:

$$\text{Heat generating rate} = \frac{Q}{(\pi/4\ D_i^2\ L)}$$ Btu/hr-in^3

where,
Q = decay heat load (24, 31.2, or 40.8 kW)
Di = inner DSC diameter = 66.19" [2]
L = DSC cavity length = 169.6" [2]

The nodes of the DSC contents are disconnected in the axial direction from the DSC shield plugs to simulate the uniform heat generation over the radial surface of the DSC.

The initial conditions for the blocked vent accident case are identical to the boundary conditions applied for the off-normal case with 105°F daily average temperature (117°F max. daylight temperature) and maximum solar heat flux. The emissivity of the support structure is set to 0.3 to remove the uncertainty about the emissivity and durability of the paints. See section 4.5 for details. The finite element model for transient runs is shown in Figure 10. The transient model simulates 48 hours of the vent blockage. This model considers only the maximum decay heat load of 40.8 kW to bound the maximum temperatures within the HSM-H for the accident conditions.

To study the maximum temperature gradients during blockage of the vents, the single HSM-H model is modified for the transient run with -40°F ambient conditions. A summary of the considered cases are shown in Table 3.

The material properties used in the models are listed in Section 4.

Table 3 – Summary of the Considered Cases for HSM-H thermal Model

Max. Decay Heat Load	Ambient Temperature	Insolance	Model	Type	Fins on Side Heat Shield
24 kW	117°F	Yes	Middle HSM-H	Steady-State	Yes
24 kW	-40°F	No	Middle HSM-H	Steady-State	Yes
31.2 kW	117°F	Yes	Middle HSM-H	Steady-State	Yes
31.2 kW	-40°F	No	Middle HSM-H	Steady-State	Yes
31.2 kW	117°F	Yes	Middle HSM-H	Steady-State	No
40.8 kW	117°F	Yes	Middle HSM-H	Steady-State	Yes
40.8 kW	100°F	Yes	Middle HSM-H	Steady-State	Yes
40.8 kW	0°F	No	Middle HSM-H	Steady-State	Yes
40.8 kW	-40°F	No	Middle HSM-H	Steady-State	Yes
40.8 kW	117°F	Yes	Middle HSM-H	Transient	Yes
40.8 kW	-40°F	No	Single / End HSM-H	Steady-State	Yes
40.8 kW	-40°F	No	Single / End HSM-H	Transient	Yes

4 – Material Properties

4.1 - Stainless Steel SA 240, type 304, DSC shell, DSC plugs – Mat 1

SA 240, Type 304	Thermal conductivity		Thermal Diffusivity	Specific heat capacity †
Temperature (°F)	(Btu/hr-ft-°F) [6]	(Btu/hr-in-°F)	(ft^2/hr) [6]	(Btu/lbm-°F)
70	8.6	0.717	0.151	0.114
100	8.7	0.725	0.152	0.114
150	9.0	0.750	0.154	0.117
200	9.3	0.775	0.156	0.119
250	9.6	0.800	0.158	0.121
300	9.8	0.817	0.160	0.122
350	10.1	0.842	0.162	0.124
400	10.4	0.867	0.165	0.126
450	10.6	0.883	0.167	0.127
500	10.9	0.908	0.170	0.128
550	11.1	0.925	0.172	0.129
600	11.3	0.942	0.174	0.130
650	11.6	0.967	0.177	0.131
700	11.8	0.983	0.179	0.132
750	12.0	1.000	0.181	0.132
800	12.2	1.017	0.184	0.132
$\rho = 0.29$ lbm/in^3 [13]				

An emissivity of 0.46 is considered for stainless steel surfaces [10].

4.2 - Concrete – HSM structure – Mat 2

The thermal conductivity of normal, saturated concrete varies from 1.2 to 2.0 Btu/ft-hr-°F at temperature ranging from 50 to 150°F [7]. The conductivity of concrete decreases rapidly with the rise in temperature and assumes, at 750°C (1382°F) a conductivity value equal approximately to 50 percent of that of normal temperature [7]. For this analysis a thermal conductivity of 1.15 Btu/hr-ft-°F (0.0958 Btu/hr-in-°F) is considered for concrete at 70°F. This conductivity is reduced by half to a value of 0.0479 Btu/hr-in-°F at 1382°F.

† Thermal diffusivity is $\alpha = \dfrac{k}{\rho\, c_p}$

The dry density of typical HSM's for NUHOMS system shall be between 145 to 152 lbm/ft^3 [8]. Practical thermal conductivity of concrete in this range is 10.0 to 16.5 $Btu/hr\text{-}ft^2\text{-}(°F/in)$ (0.0694 to 0.1145 Btu/hr-in-°F) [9]. This shows that the assumed concrete conductivity is within this range and therefore acceptable.

The specific heat of concrete is considered to be 0.22 Btu/lbm-°F in this analysis.

Emissivity of concrete is reportedly 0.9 t0 0.94 [5 and 11]. An emissivity of 0.90 is considered for concrete surfaces in this analysis.

4.3 - Soil – Mat 3

The following properties are considered for soil in this analysis:
Thermal conductivity = 0.3 W/m-K (0.0144 Btu/hr-in-°F) [11]
Density = 1600 kg/m3 (0.0578 lbm/in^3) [11]
Specific heat = 800 J/kg-°C (0.191 Btu/lbm-°F) [11]

4.4 – Aluminum 1100 – side and top shields – Mat 4

Al 1100	Thermal conductivity		Thermal Diffusivity	Specific heat capacity‡
Temperature (°F)	(Btu/hr-ft-°F) [6]	(Btu/hr-in-°F)	(ft^2/hr) [6]	(Btu/lbm-°F)
70	133.1	11.092	3.67	0.214
100	131.8	10.983	3.61	0.216
150	130.0	10.833	3.50	0.219
200	128.5	10.708	3.42	0.222
250	127.3	10.608	3.35	0.224
300	126.2	10.517	3.28	0.227
350	125.3	10.442	3.23	0.229
400	124.5	10.375	3.17	0.232
ρ = 0.098 lbm/in^3 [8]				

Emissivity of anodized aluminum is reported to be 0.88 to 0.94 [5 and 12] at moderate temperatures and decreases rapidly at high temperatures. An emissivity of 0.80 is considered for anodized surfaces in this analysis to cover the expected temperature range. Emissivity of not anodized aluminum surfaces is set to 0.1 [13].

‡ Thermal diffusivity is $\alpha = \dfrac{k}{\rho\, c_P}$

4.5 - Steel – Support structure – Mat 6

Carbon Steel	Thermal conductivity		Thermal Diffusivity	Specific heat capacity [§]
Temperature (°F)	(Btu/hr-ft-°F) [6]	(Btu/hr-in-°F)	(ft^2/hr) [6]	(Btu/lbm-°F)
70	35.1	2.925	0.695	0.103
100	34.7	2.892	0.674	0.105
200	33.6	2.800	0.613	0.112
300	32.3	2.692	0.561	0.117
400	30.9	2.575	0.512	0.123
500	29.5	2.458	0.472	0.127
600	28.0	2.333	0.433	0.132
700	26.6	2.212	0.394	0.138
800	25.2	2.100	0.355	0.145
900	23.8	1.983	0.317	0.153
1000	22.4	1.867	0.282	0.162
ρ = 0.284 lbm/in^3 [13]				

The external surfaces of the support structure might be painted. The thermal analysis uses an emissivity of 0.9 for the support structure surfaces. A sensitivity analysis is performed in Appendix C to investigate the thermal effects of the support structure emissivity value,.

4.6 – Effective Basket Properties for NUHOMS-24PTH (Mat 11)

Basket is modeled as homogenized material for the transient models. The effective basket density is 0.0912 lbm/in^3 as reported in [18]. The effective thermal conductivity and effective specific heat values are calculated for the NUHOMS-24PTH basket in [19]. The minimum values for a basket with inserts and 40.8 kW decay heat load are as follows.

Temperature (°F)	k_{eff} Transverse (Btu/min-in-°F) [19]	Temperature (°F)	k_{eff} Axial (Btu/min-in-°F) [19]	Temperature (°F)	Cp,eff (Btu/lbm-°F) [19]
248	3.676E-03	200	4.197E-04	100	0.1052
338	3.949E-03	300	4.428E-04	200	0.1092
427	4.275E-03	400	4.659E-04	300	0.1127
518	4.615E-03	500	4.851E-04	400	0.1152
610	4.958E-03	600	5.044E-04	1000	0.1208
703	5.292E-03	800	5.467E-04		
799	5.522E-03				
897	5.618E-03				

[§] Thermal diffusivity is $\alpha = \dfrac{k}{\rho\, c_P}$, this equation is used to calculate the specific heat

4.7 - Air (Mat 7 and 12)

The following conductivity values are considered for air in the model.

Temperature		Thermal Conductivity of Air	
(K) [14]	(°F)	(W/m-K) [14]	(Btu/hr-in-°F)
100	-280	0.0093	0.0004
200	-100	0.0181	0.0009
300	80	0.0263	0.0013
400	260	0.0336	0.0016
500	440	0.0404	0.0019
600	620	0.0466	0.0022
800	980	0.0577	0.0028
1000	1340	0.0681	0.0033

The specific heat capacity and the density of gases are very small in comparison to metal components. These values are set to zero in model for simplification.

Material number 7 is considered for the shell elements on the symmetry plane. The emissivity of these elements is set to 0.001.

4.8 – Effective Air Conductivity in the closed cavity of the HSM-H (Mat 10)

During blockage of the inlet and outlet vents, the air within the HSM-H is trapped. The convection heat transfer under these circumstances reduces to free convection in closed cavities. To simplify the model, an effective conductivity for air is calculated, which includes the conduction and convection heat transfer through the air in the closed cavity of the HSM-H.

Reference [14] introduces the following correlation to calculate the conduction and convection heat transfer in closed cavities for eccentric horizontal cylinders.

$$Nu = [Nu_{COND}, Nu_l]_{max} \qquad (1)$$

With

q' = heat transfer by conduction and convection from the inner cylinder to the outer one per unit axial length of cylinder

$$Nu_{COND} = \frac{\ln(D_o / D_i)}{\cosh^{-1}[(D_o^2 + D_i^2 - 4E^2)/2D_oD_i]}$$

$$Nu_l = 0.603\overline{C}_l \frac{(\ln D_o/D_i)\,Ra^{1/4}}{[(L/D_i)^{3/5} + (L/D_o)^{3/5}]^{5/4}}$$

where,

$$Ra = \frac{g\beta(T_i - T_o)L^3}{\nu^2} \times \Pr \quad \text{with} \quad L = (D_o - D_i)/2 \text{ and}$$

$$\overline{C}_l = \tfrac{4}{3}\frac{0.503}{[1+(0.492/\Pr)^{9/16}]^{4/9}}$$

The geometry and dimensions to use in the correlations are shown in the following figure.

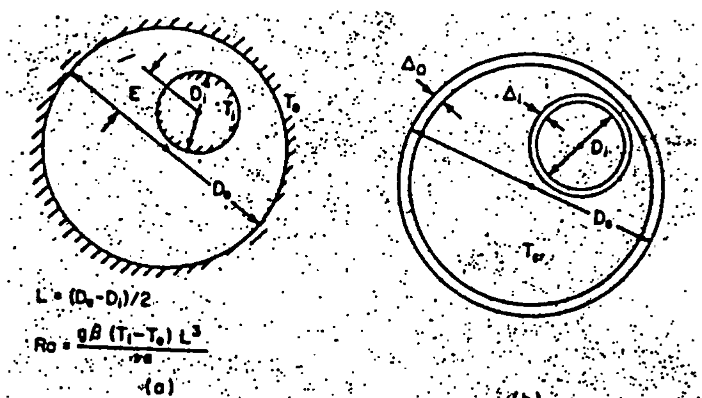

Sketch of concentric and eccentric cylinder and sphere problems. [14]

The Nu number in correlation (1) is defined as

$$Nu = \frac{q'\ln(D_o/D_i)}{2\pi(T_i - T_o)k}$$

This implements that the air effective conductivity is equal to the product of Nu and the air conductivity for the closed cavity between cylinders.

$$k_{eff} = Nu\ k_w$$

k_{eff} = effective conductivity for conduction and convection from inner to outer cylinder
k = conductivity of air

All air properties are evaluated at average temperature.

$$T_{avg} = (T_o + T_i)/2$$

In order to use the above correlations for the HSM-H cavity, a hydraulic diameter is calculated for the cross section of the HSM-H cavity surrounded by the side and top shields.

$$D_{h,HSM} = \frac{4A}{P} = \frac{4\times(82.375\times168)}{2\times(82.375+168)} = 115"$$

The effective conductivity defined in the above correlations depends on the inner cylinder and outer cylinder temperatures (T_i and T_o) and its gradient. A study of the effect of T_i and T_o on the effective conductivity of air in the closed cavity of the HSM-H is shown in Table 4. In the study, the inner temperature T_i varies from 425°F to 825°F, which represents the DSC shell temperature during blockage of the vents. The outer temperature T_o varies from 150°F to 350°F, which represents the shield or the concrete temperatures. The gradient between T_i and T_o varies from 275°F to 475°F. The calculated effective conductivity of air for all of the studied cases is 0.05 Btu/hr-in-°F.

The minimum temperature gradient observed in the model occurs between the middle of the side heat shield and the DSC side. The minimum gradient after 40 hour blockage of the vents is:
574 (DSC side) – 451 (side heat shield) = 123°F

The maximum temperature gradient occurs between the uncovered top corner of the HSM-H and top of the DSC shell. The maximum gradient after 40 hour blockage of the vents is:
581 (DSC side) – 214 (side heat shield) = 367°F

The temperature gradients covered in the study are higher than the gradients observed after solving the model. Nonetheless using the calculated value of 0.05 Btu/hr-in-°F for effective air conductivity is acceptable since the concrete temperature is the limiting factor in the blocked vent thermal analysis. Using a higher temperature gradient, which results in a higher air effective conductivity value, increases the heat transfer from the DSC shell to the concrete walls and causes a higher concrete temperature during blockage of the vents.

The air properties used for calculation of the air effective conductivity are listed in Table 5.

Table 4 – Effective Conductivity of Air in the Closed HSM-H Cavity

	(in)	(m)		(in)	(m)
Di =	67.19	1.707	E =	13	0.330
Do =	115.0	2.920	L =	23.9	0.607

Ti	To	T_{avg}	T_{avg}	k	β	ν	Pr	C_l	Ra	Nu_{COND}	Nu_l	Nu	k_eff
(F)	(F)	(F)	(K)	(W/m-K)	(1/K)	(m^2/s)	(---)	(---)	(---)	(---)	(---)	(---)	(Btu/hr-in-F)
825	350	588	582	0.045	1.73E-03	5.02E-05	0.69	0.513	2.73E+08	1.00	23.5	23.5	0.05
775	350	563	568	0.045	1.77E-03	4.83E-05	0.69	0.513	2.71E+08	1.00	23.4	23.4	0.05
725	350	538	554	0.044	1.82E-03	4.63E-05	0.69	0.513	2.67E+08	1.00	23.3	23.3	0.05
675	350	513	540	0.043	1.87E-03	4.44E-05	0.69	0.513	2.58E+08	1.00	23.1	23.1	0.05
625	350	488	526	0.042	1.91E-03	4.25E-05	0.69	0.513	2.44E+08	1.00	22.8	22.8	0.05
775	300	538	554	0.044	1.82E-03	4.63E-05	0.69	0.513	3.38E+08	1.00	24.8	24.8	0.05
725	300	513	540	0.043	1.87E-03	4.44E-05	0.69	0.513	3.37E+08	1.00	24.7	24.7	0.05
675	300	488	526	0.042	1.91E-03	4.25E-05	0.69	0.513	3.33E+08	1.00	24.7	24.7	0.05
625	300	463	513	0.041	1.96E-03	4.05E-05	0.69	0.513	3.25E+08	1.00	24.5	24.5	0.05
575	300	438	499	0.040	2.01E-03	3.86E-05	0.69	0.513	3.10E+08	1.00	24.2	24.2	0.05
725	250	488	526	0.042	1.91E-03	4.25E-05	0.69	0.513	4.22E+08	1.00	26.2	26.2	0.05
675	250	463	513	0.041	1.96E-03	4.05E-05	0.69	0.513	4.25E+08	1.00	26.2	26.2	0.05
625	250	438	499	0.040	2.01E-03	3.86E-05	0.69	0.513	4.23E+08	1.00	26.2	26.2	0.05
575	250	413	485	0.039	2.08E-03	3.69E-05	0.69	0.513	4.16E+08	1.00	26.1	26.1	0.05
525	250	388	471	0.038	2.15E-03	3.52E-05	0.69	0.513	4.01E+08	1.00	25.8	25.8	0.05
675	200	438	499	0.040	2.01E-03	3.86E-05	0.69	0.513	5.36E+08	1.00	27.8	27.8	0.05
625	200	413	485	0.039	2.08E-03	3.69E-05	0.69	0.513	5.44E+08	1.00	27.9	27.9	0.05
575	200	388	471	0.038	2.15E-03	3.52E-05	0.69	0.513	5.46E+08	1.00	27.9	27.9	0.05
525	200	363	457	0.037	2.22E-03	3.34E-05	0.69	0.513	5.41E+08	1.00	27.9	27.9	0.05
475	200	338	443	0.037	2.28E-03	3.17E-05	0.69	0.513	5.25E+08	1.00	27.7	27.7	0.05
625	150	388	471	0.038	2.15E-03	3.52E-05	0.69	0.513	6.92E+08	1.00	29.6	29.6	0.05
575	150	363	457	0.037	2.22E-03	3.34E-05	0.69	0.513	7.07E+08	1.00	29.8	29.8	0.05
525	150	338	443	0.037	2.28E-03	3.17E-05	0.69	0.513	7.16E+08	1.00	29.9	29.9	0.05
475	150	313	429	0.036	2.35E-03	3.00E-05	0.69	0.513	7.16E+08	1.00	29.9	29.9	0.05
425	150	288	415	0.035	2.42E-03	2.83E-05	0.69	0.513	7.02E+08	1.00	29.7	29.7	0.05

Table 5 – Air Properties [14]

Temperature	v	Conductivity	Prandtl	Dyn. Visc.
(K)	(m3/kg)	(W/m-K)	(-----)	(Pa-s)
200	0.573	0.0181	0.740	1.33E-05
300	0.861	0.0263	0.708	1.85E-05
400	1.148	0.0336	0.694	2.30E-05
500	1.436	0.0404	0.688	2.70E-05
600	1.723	0.0466	0.690	3.06E-05
800	2.298	0.0577	0.705	3.70E-05
1000	2.872	0.0681	0.707	4.24E-05

Temperature	ρ	Conductivity	Prandtl	Kin. Visc.
(F)	(lbm/ft^3)	(Btu/hr-ft-F)	(-----)	(ft^2/hr)
-100	0.109	0.0105	0.740	0.2953
80	0.073	0.0152	0.708	0.6172
260	0.054	0.0194	0.694	1.0232
440	0.043	0.0233	0.688	1.5024
620	0.036	0.0269	0.690	2.0430
980	0.027	0.0333	0.705	3.2948
1340	0.022	0.0393	0.707	4.7187

5 – Results and Conclusion

Temperature distributions for the normal and off-normal cases are show in Figures 11 to 19. The maximum component temperatures for the normal and off-normal cases are listed below.

	24 kW		31.2 kW		
	Max. Temp. (°F)		Max. Temp. (°F)		
Component	Amb. 117°F With fins	Amb. -40°F With fins	Amb. 117°F With fins	Amb. -40°F With fins	Amb. 117°F Without fins
DSC Shell	344	216	391	270	401
Concrete	168	-2	183	9	201
Top shield	162	0	173	8	176
Side Shield	152	-9	164	1	221
Support Rail	221	71	248	99	254

	40.8 kW			
	Max. Temp. (°F)			
Component	Amb. 117°F With fins	Amb. 100°F With fins	Amb. 0°F With fins	Amb. -40°F With fins
DSC Shell	448	445	367	333
Concrete	202	197	76	25
Top shield	188	182	65	18
Side Shield	181	175	60	14
Support Rail	280	276	177	135

The above table shows that the HSM-H temperatures without the fins on the side heat shield for 31.2 kW are bounded by the case with the fins for 40.8 kW decay heat load.

Appendix C shows that decreasing the support structure emissivity from 0.9 to 0.3 affects the temperature distribution in HSM-H insignificantly. All the maximum component temperatures are increased by less than 1°F except for the support structure. The maximum temperature of the support structure increases by 17°F from 280°F to 297°F in the worst case. The maximum temperature of the support structure may be conservatively considered at 297°F or higher for further analysis of the HSM-H. The effects of the offset sidewall and slightly higher bulk temperatures on the temperature profiles of the HSM-H components are insignificant as shown in Appendix C.

Temperature distributions for the blocked vent accident case with 40.8 kW decay heat load 38.5 hours after blockage of the vents are shown in Figure 20. The maximum component temperatures for the blocked vent accident case are listed below.

	Max. Temp. (°F)			
	40.8 kW decay heat load - 117°F ambient			
Component	Initial Temp**	36 hr blockage	38.5 hr blockage	40 hr blockage
DSC Shell	440	572	578	581
Concrete	202	396	406	411
Top shield	187	306	313	317
Side Shield	180	438	446	451
Support Rail	318	524	530	533

Figure 21 shows the time-temperature history of selected components from HSM-H during blockage of vents.

Temperature distributions for the single HSM-H (max. temperature gradients) are shown in Figures 22 and 23. The maximum component temperatures for these cases are listed below.

Single HSM-H	40.8 kW, -40°F ambient	40.8 kW, -40°F ambient Transient (Blocked Vents)			
	Max. Temp. (°F)	Max. Temp. (°F)			
Component	Steady-State	Initial Temp	36 hr blockage	38.5 hr blockage	40 hr blockage
DSC Shell	333	322	481	486	489
Concrete	20	28	225	234	(239)
Top shield	18	18	114	119	122
Side Shield	14	12	283	291	296
Support Rail	135	172	429	434	437

** The initial temperatures are different from the values reported for the steady-state analysis due to the following differences between the steady-state and transient models:

a) Steady-state model has a finer mesh size
b) Emissivity of support rail in transient model is 0.3 as oppose to steady-state model which is 0.9
c) Heat generating boundary conditions are used in transient model as oppose to heat fluxes used in the steady-state model

Figure 1 – Air Flow Diagram

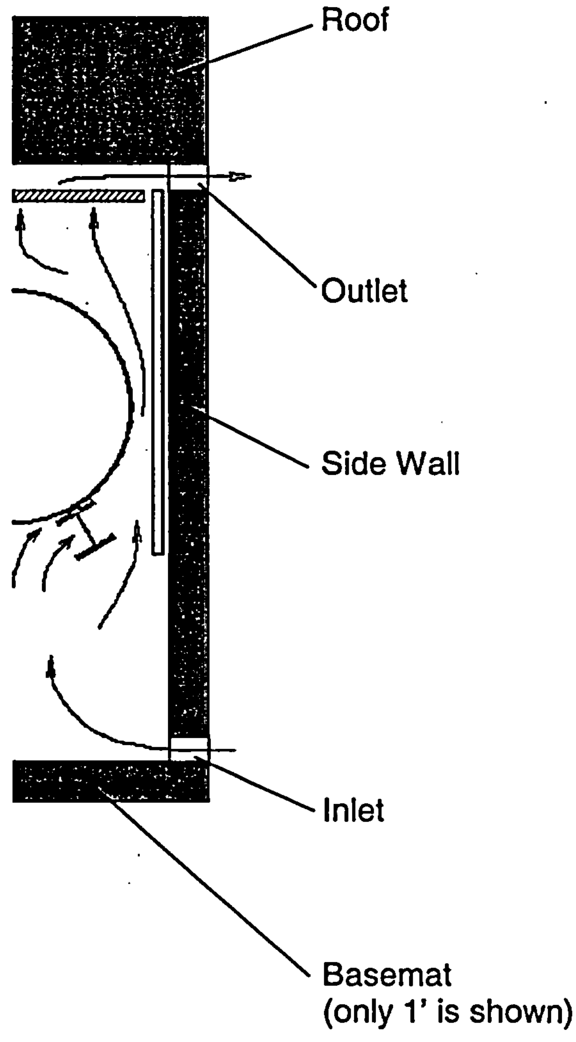

Figure 2 – Finite Element Model – Entire Model

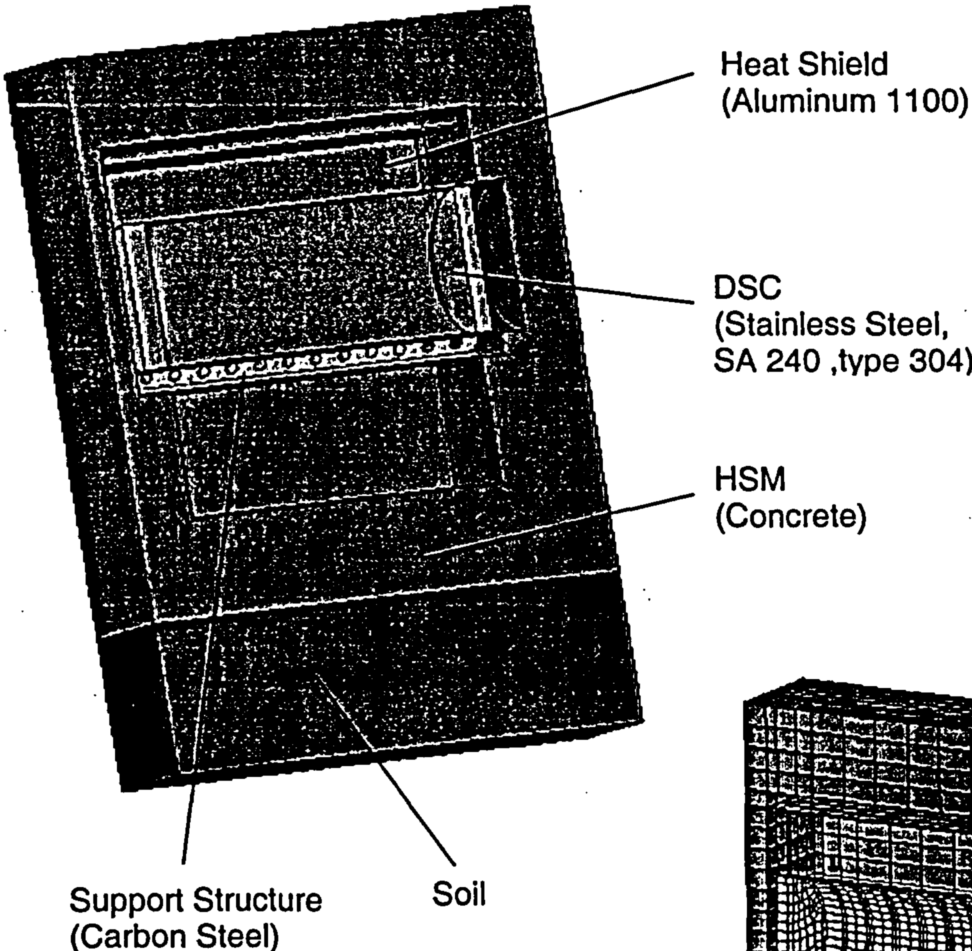

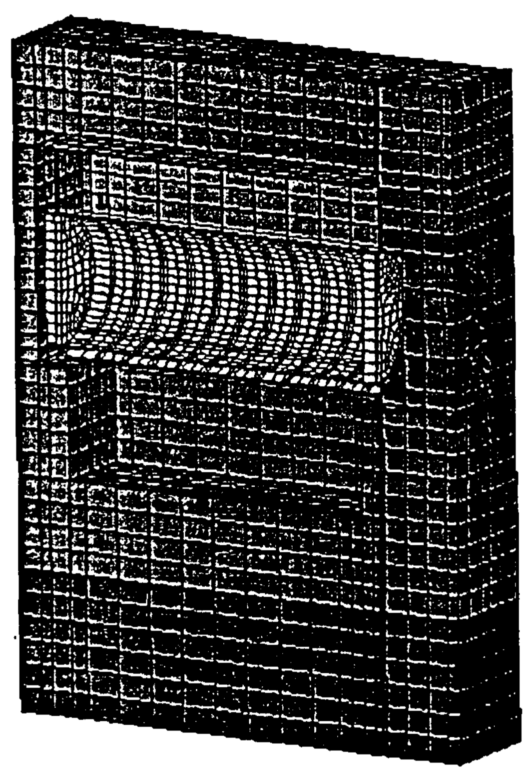

Figure 3 - Finite Element Model – DSC and Support Structure

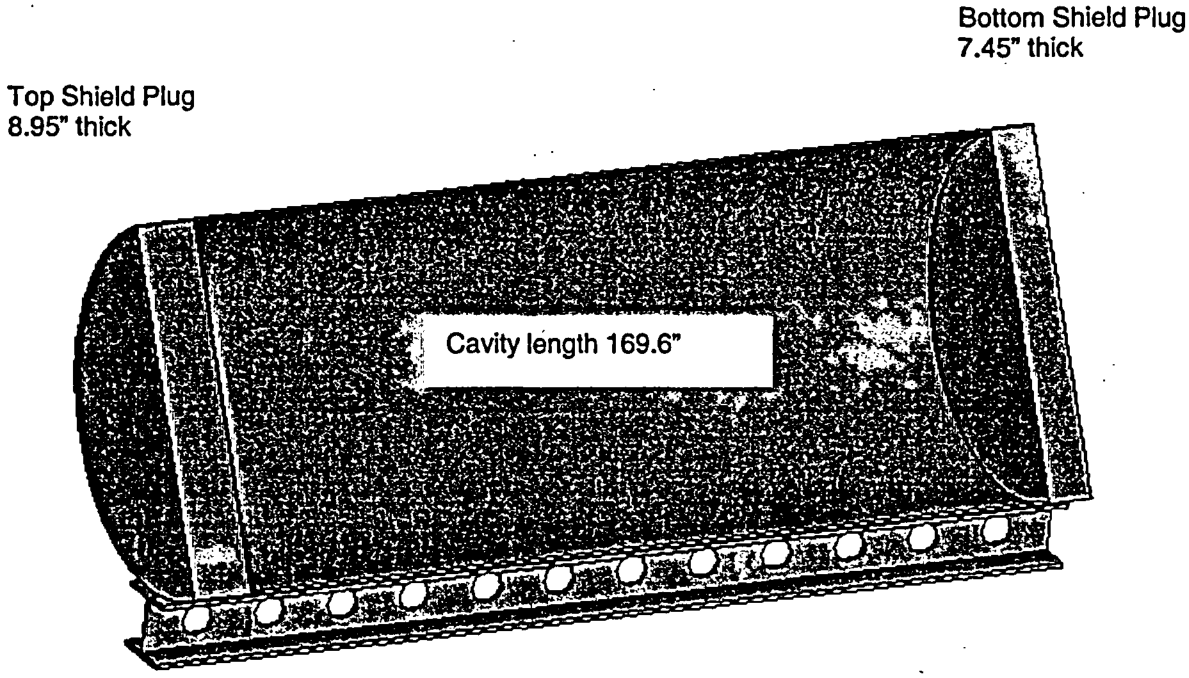

Figure 4 – Finite Element Model – Concrete Structure

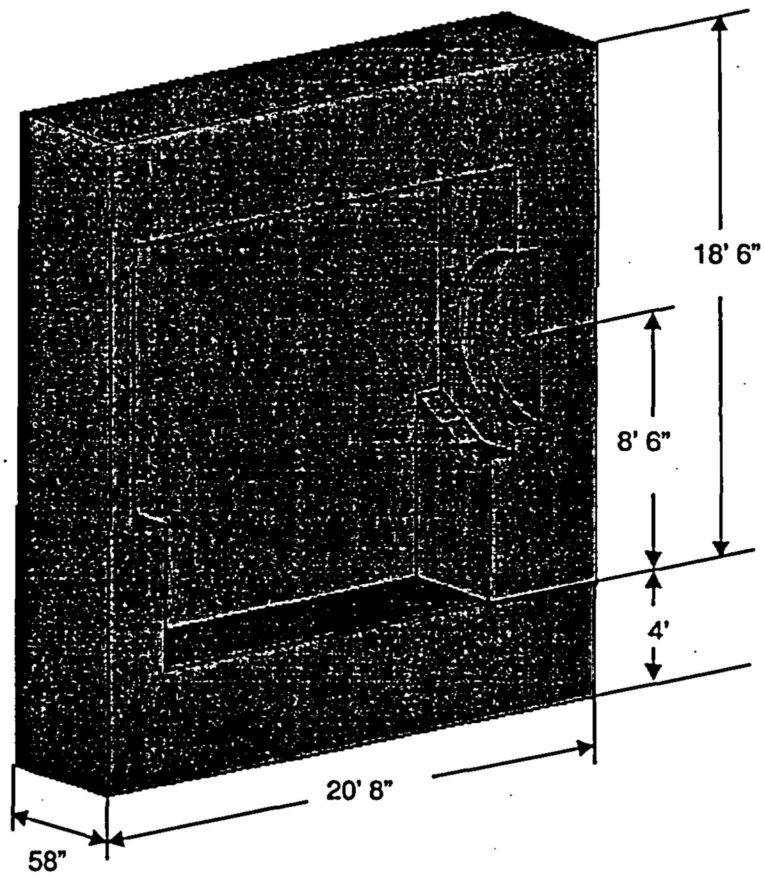

Figure 5 – Finite Element Model – Heat Shields

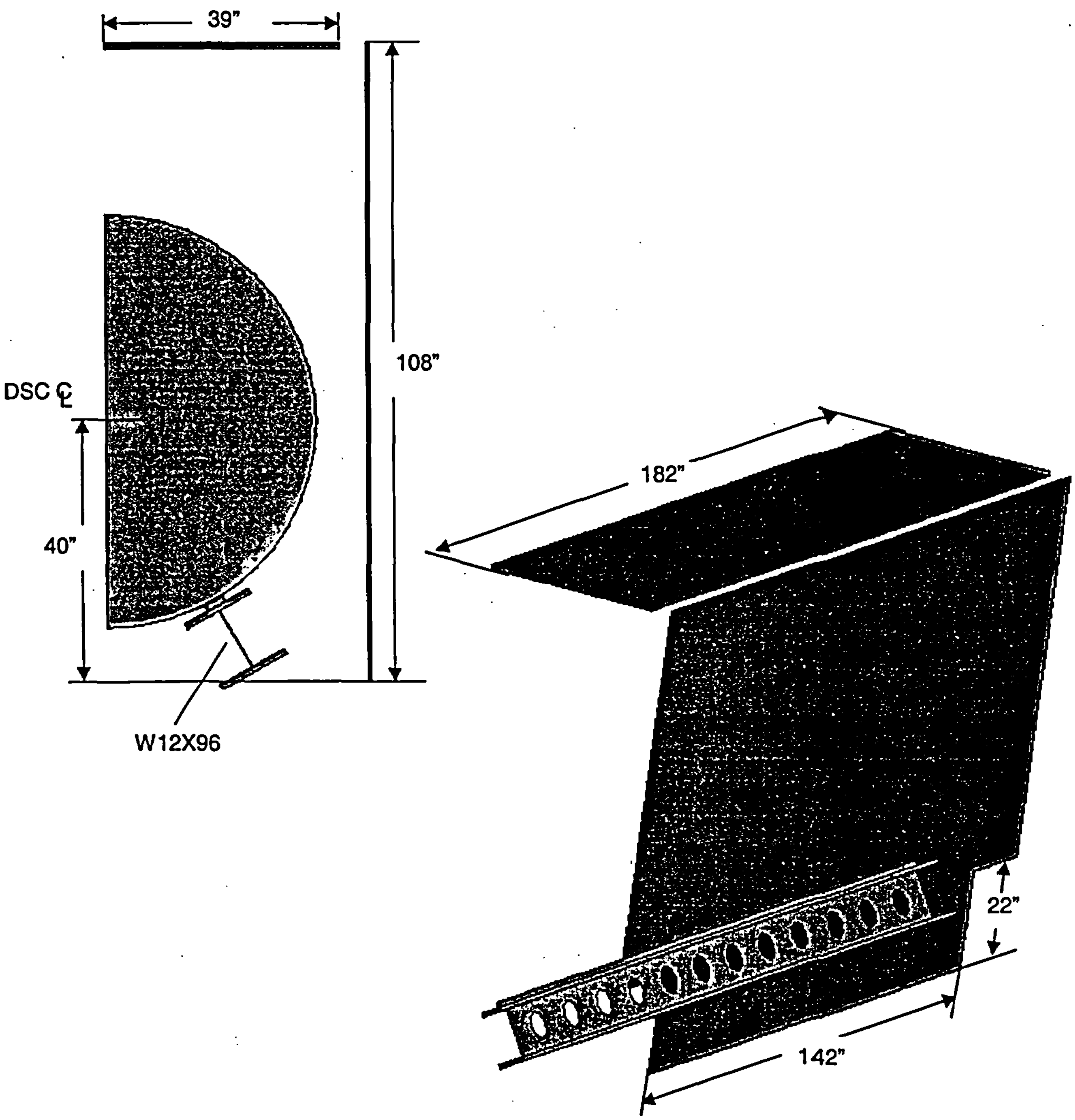

Figure 6 – DSC Convection

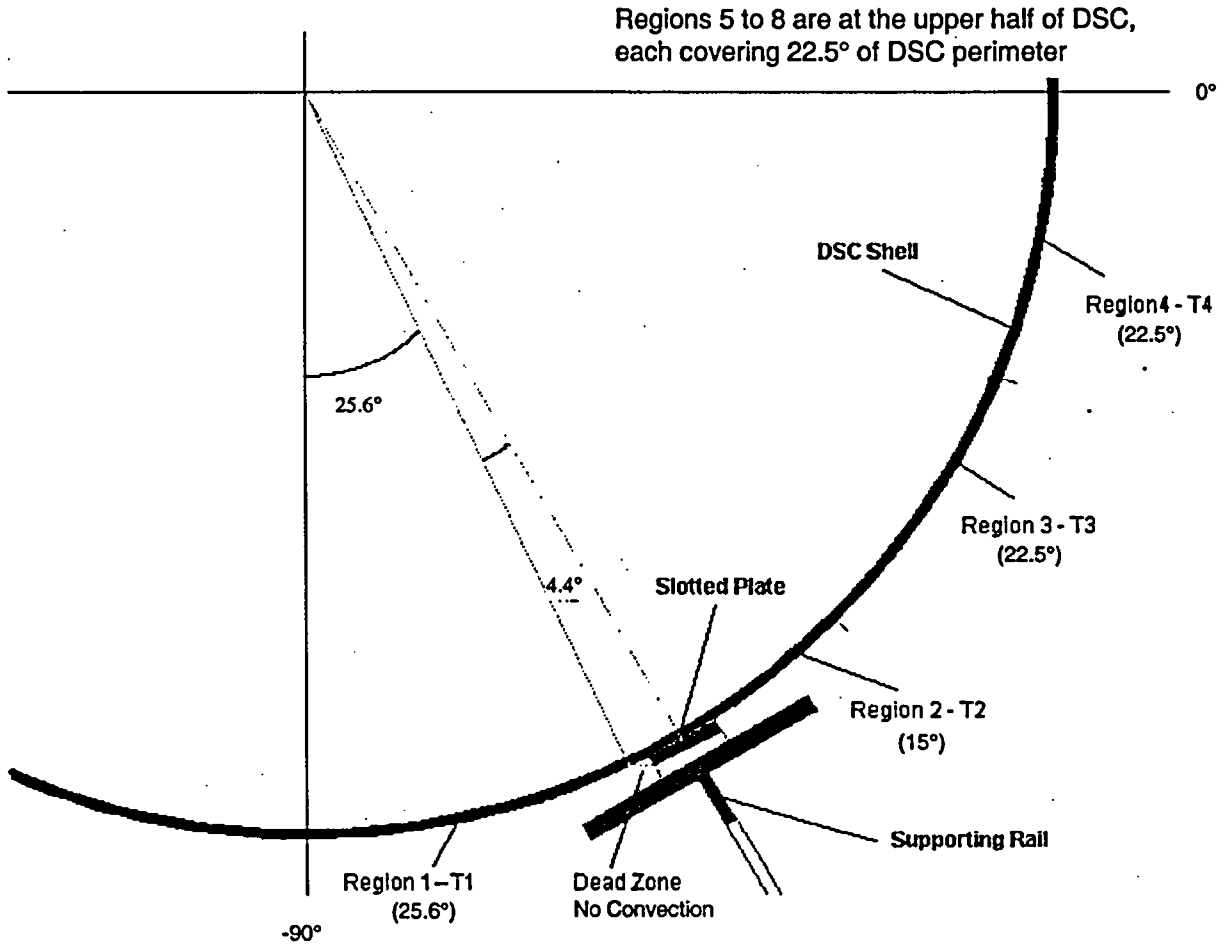

Figure 7 – Finite element Model of a Single HSM-H

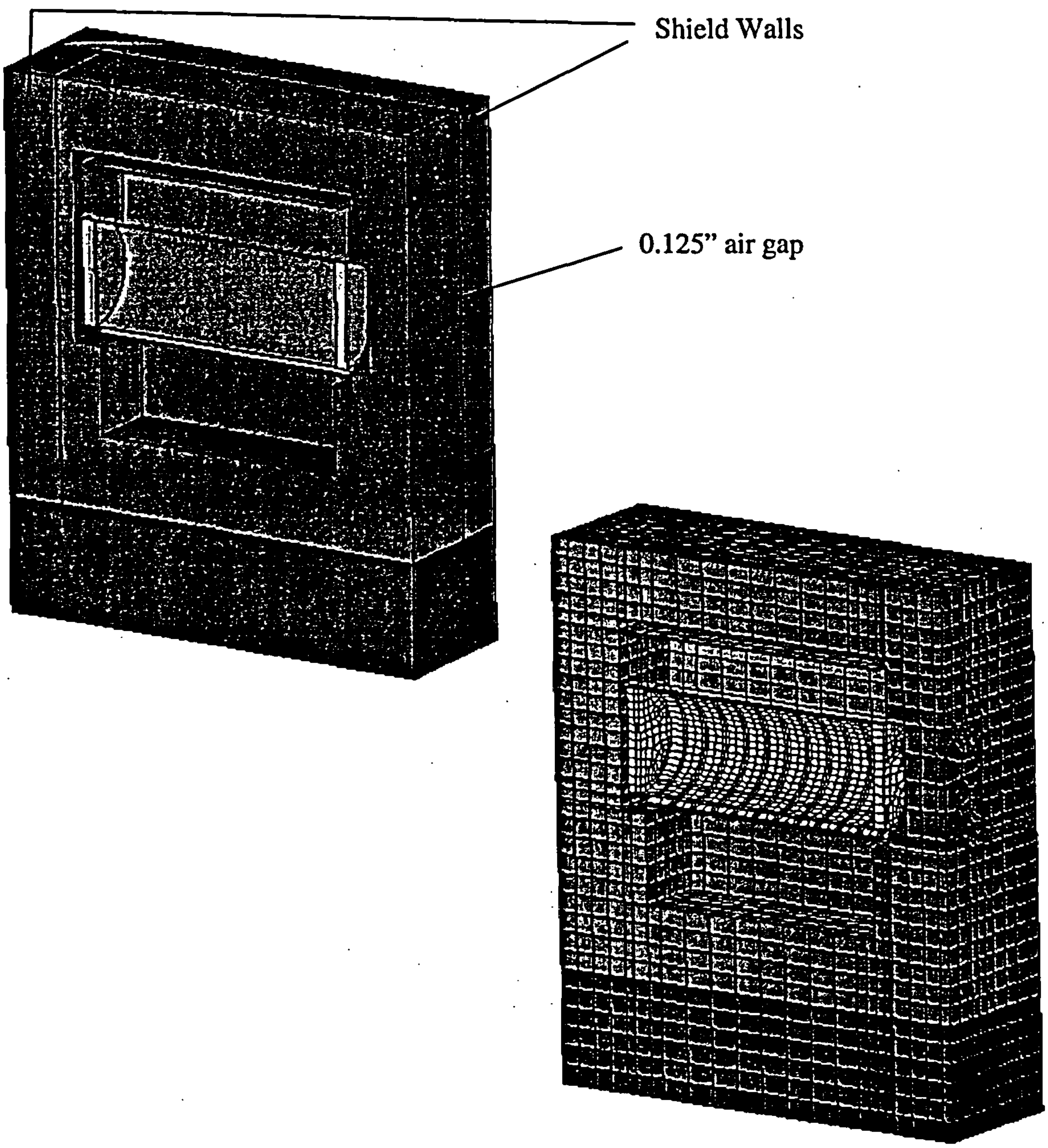

Figure 8 – Convection Boundary Conditions for Maximum Ambient temperature

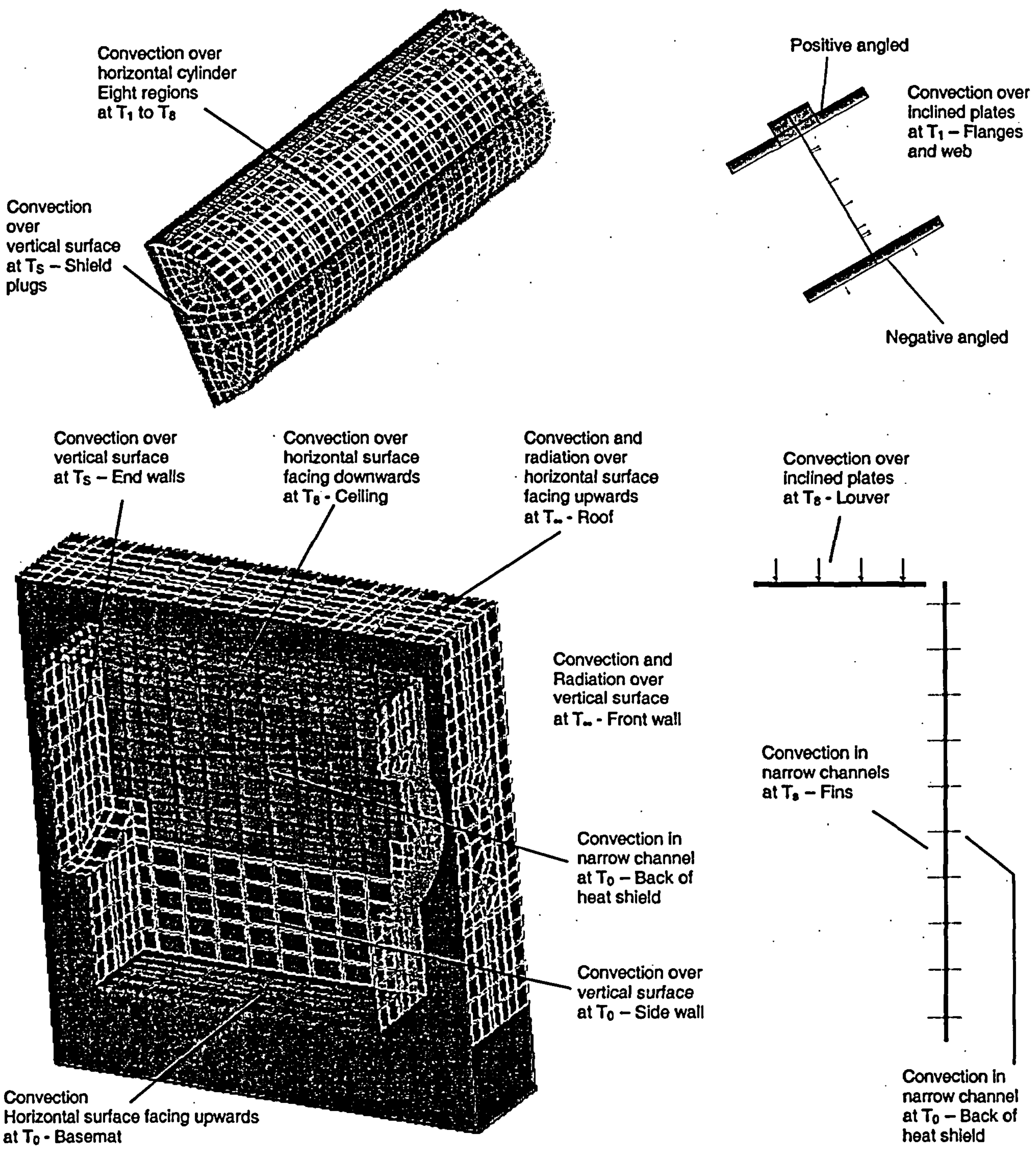

Figure 9 – Heat Flux and Fixed Temperature Boundary Conditions for Maximum Ambient Temperature

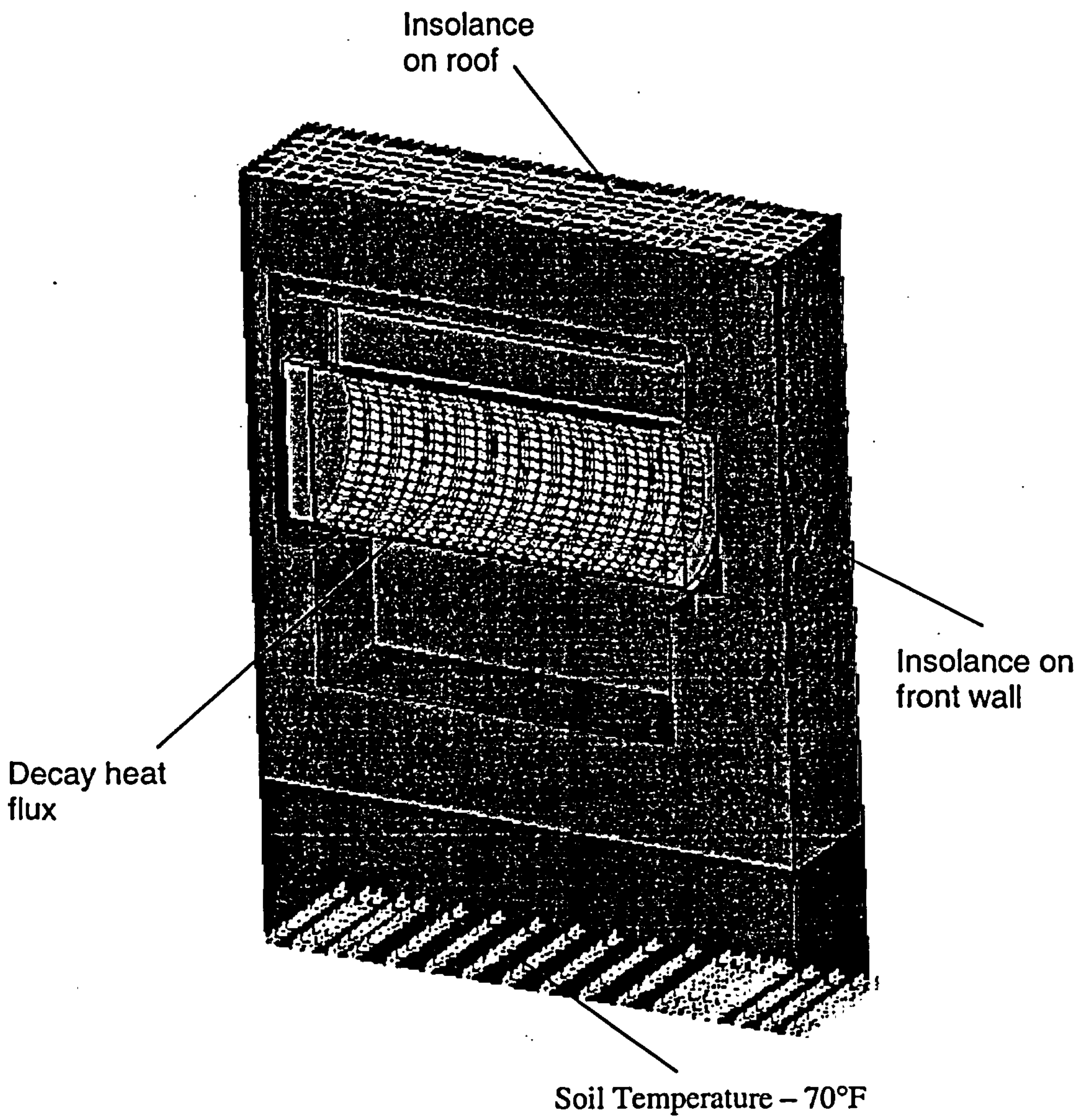

Figure 10 – Finite Element Model for the Blocked vent Accident Case

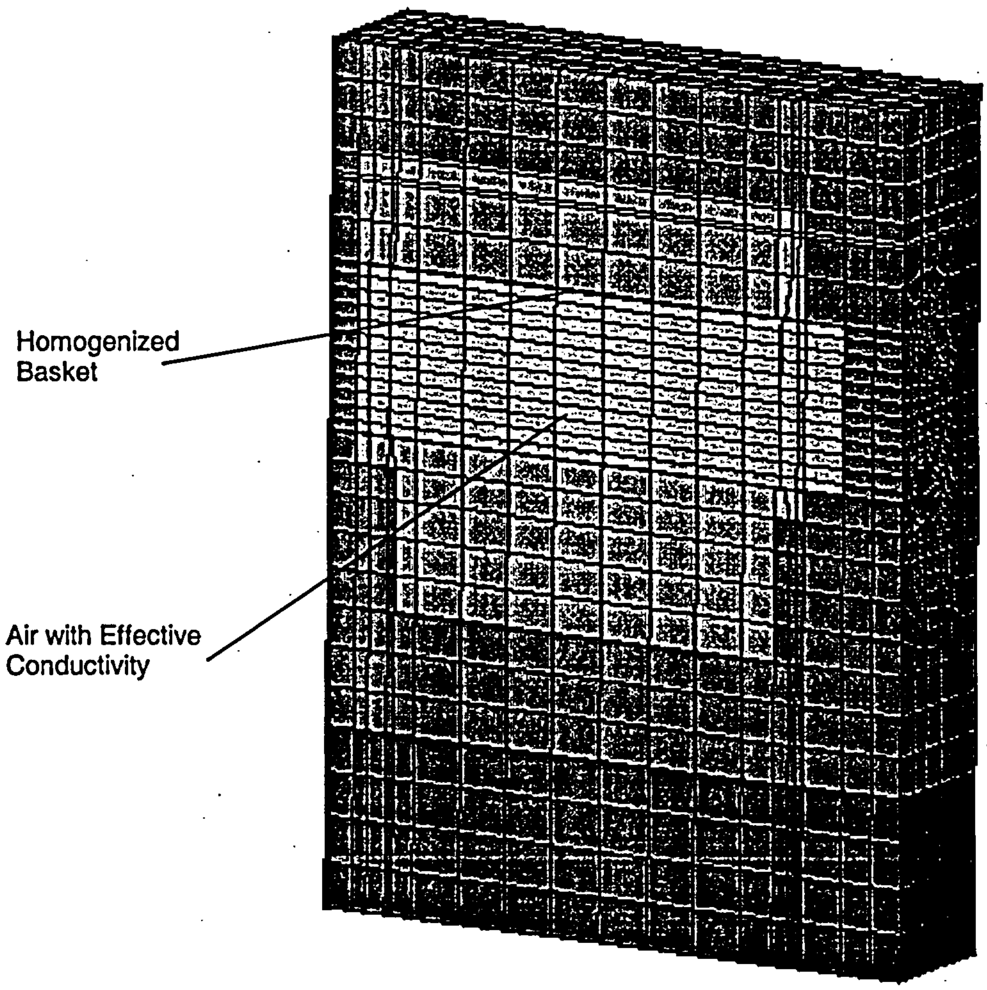

Figure 11 – Temperature Distribution – 24kW, 117°F Ambient

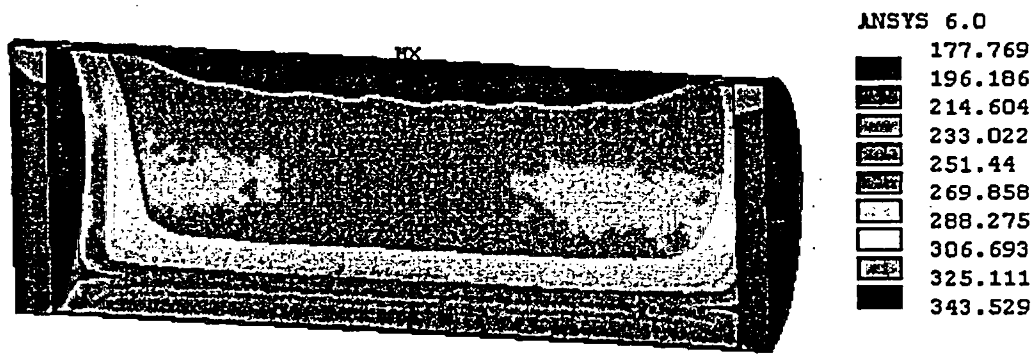

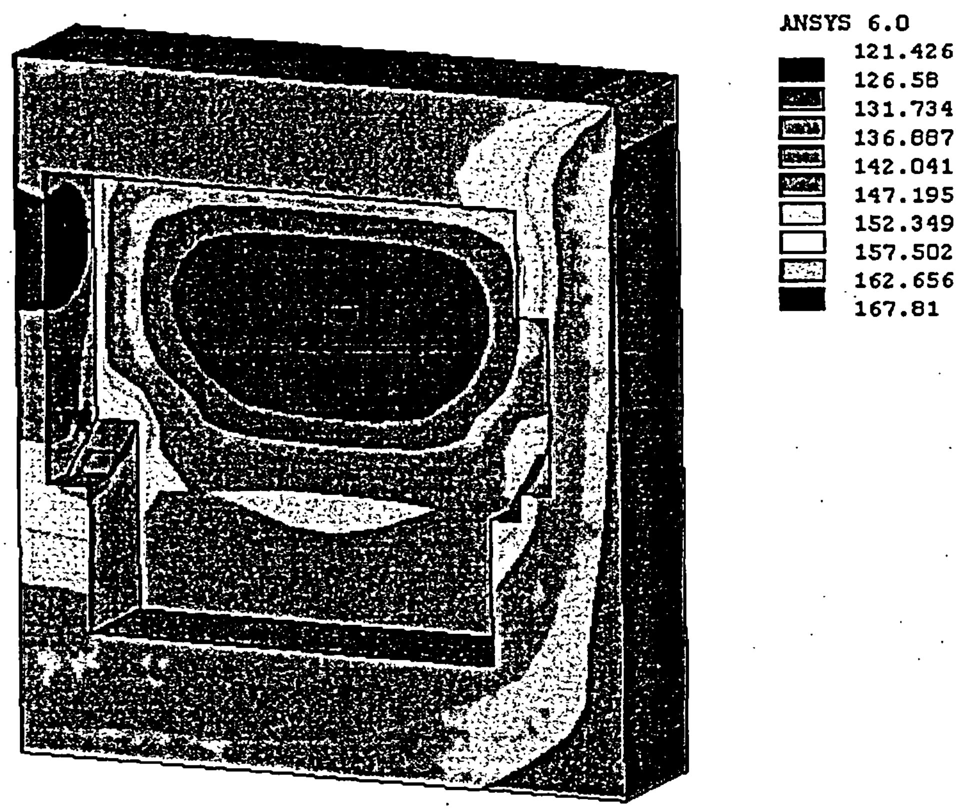

Figure 12 – Temperature Distribution – 24kW, -40°F Ambient

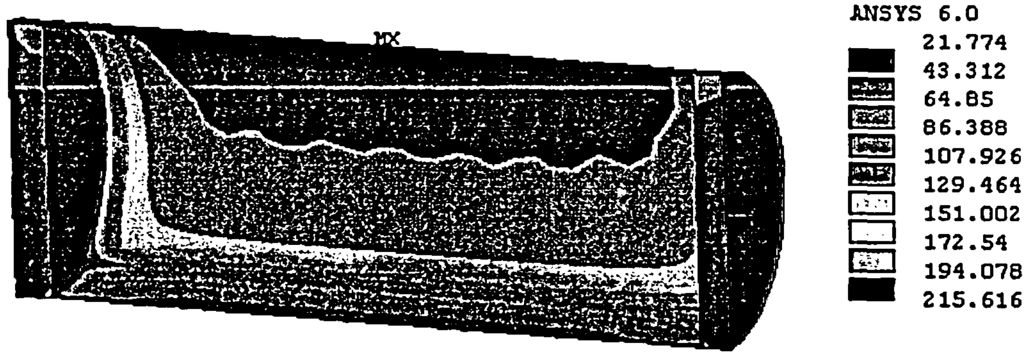

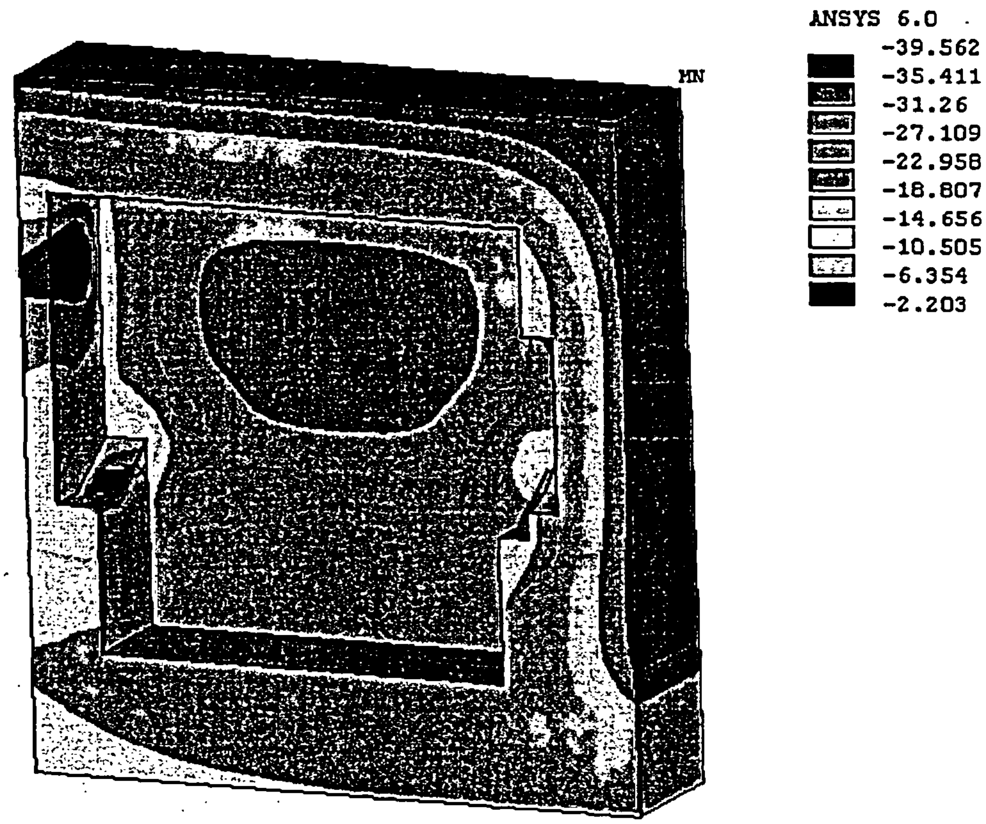

TRANSNUCLEAR, INC.

CALC. NO 60977-03

REV. 0

TITLE NUHOMS-24PTH, Thermal Analysis of the HSM Storage Conditions

Figure 13 – Temperature Distribution – 31.2kW, 117°F Ambient

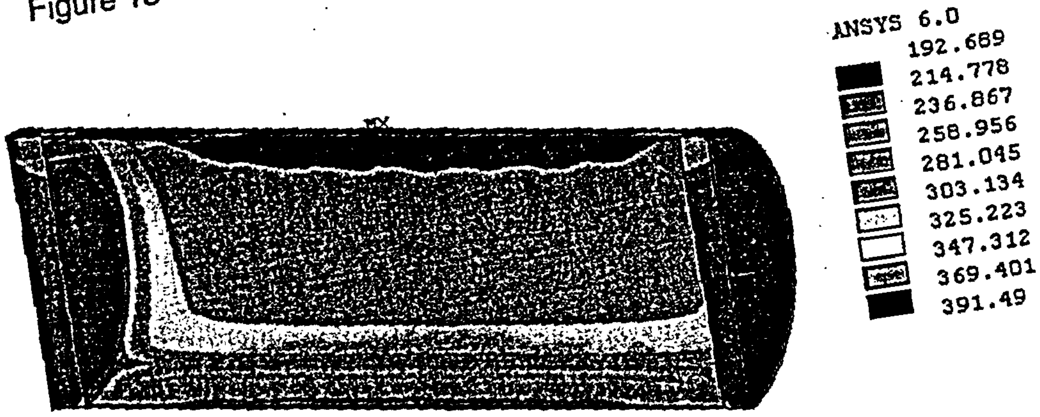

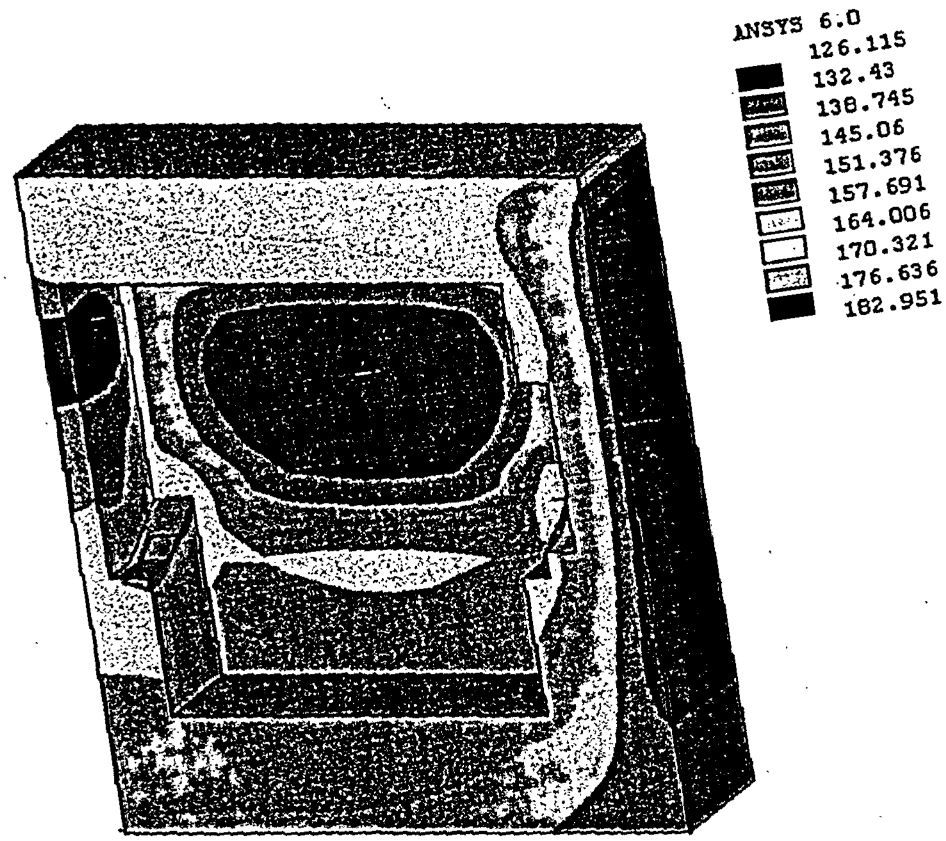

Figure 14 – Temperature Distribution – 31.2kW, -40°F Ambient

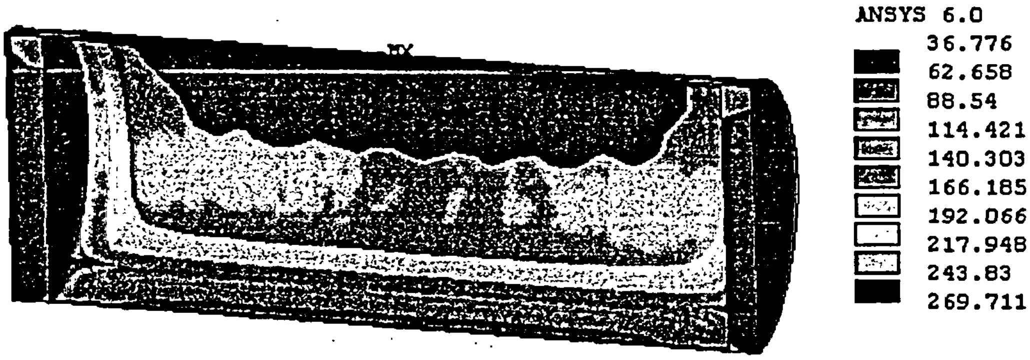

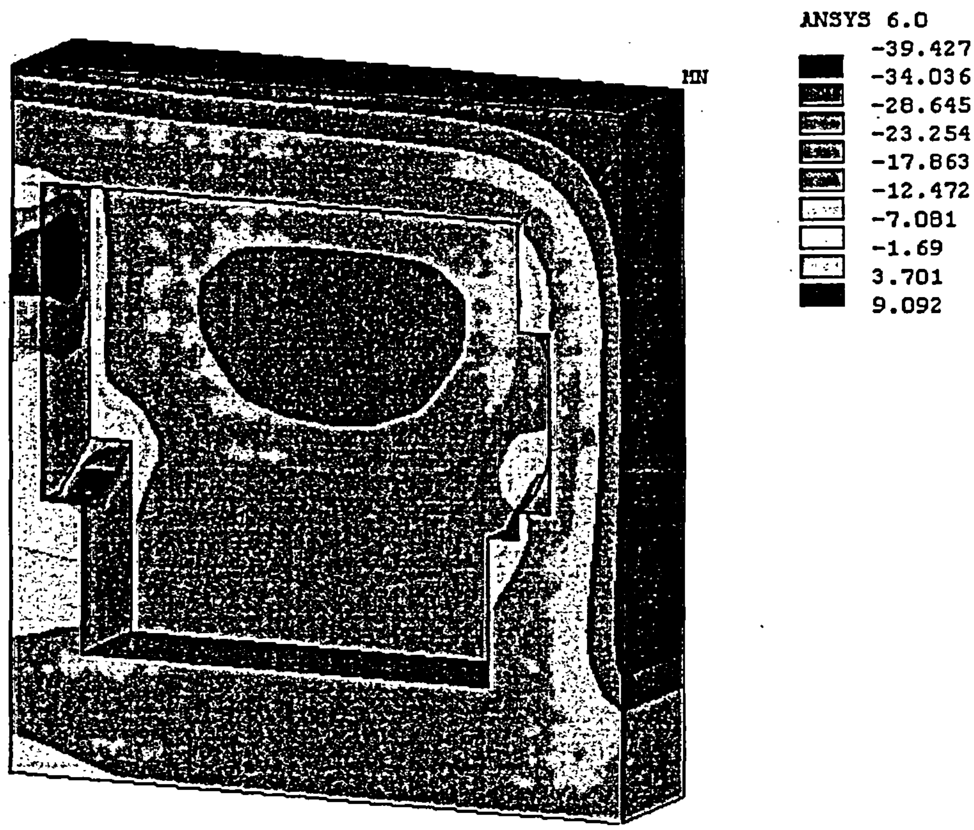

Figure 15 – Temperature Distribution – 31.2kW, 117°F Ambient, Without Fins on the Side Heat shield

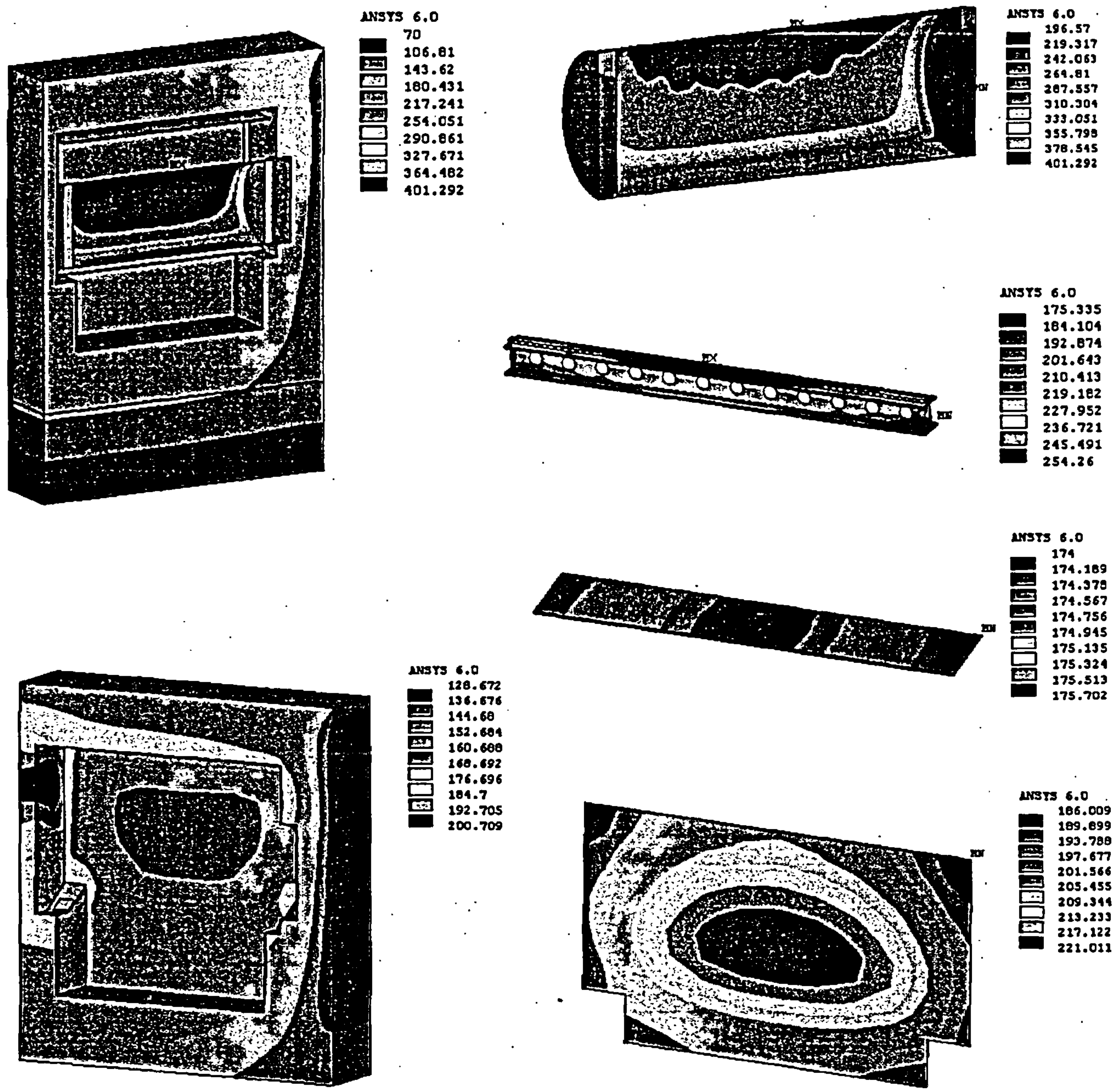

Figure 16 – Temperature Distribution – 40.8kW, 117°F Ambient

DSC

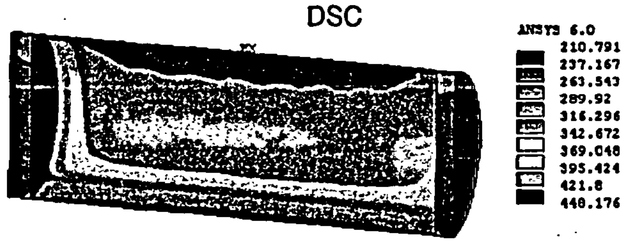

Top Heat Shield

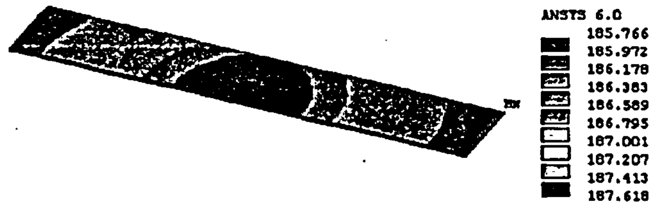

Support Rail

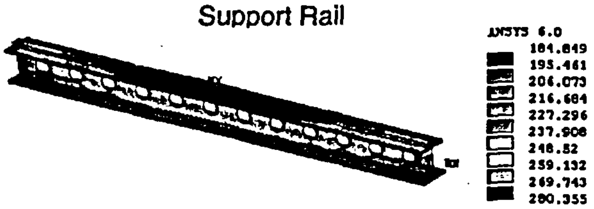

Side Heat Shield

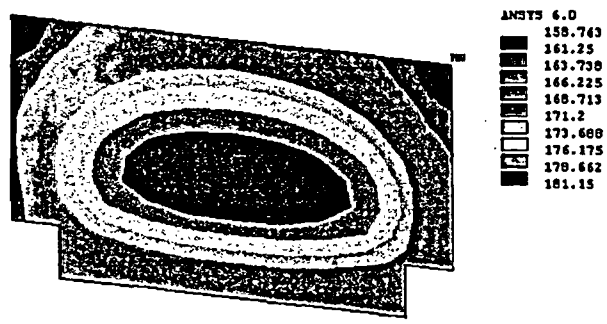

HSM

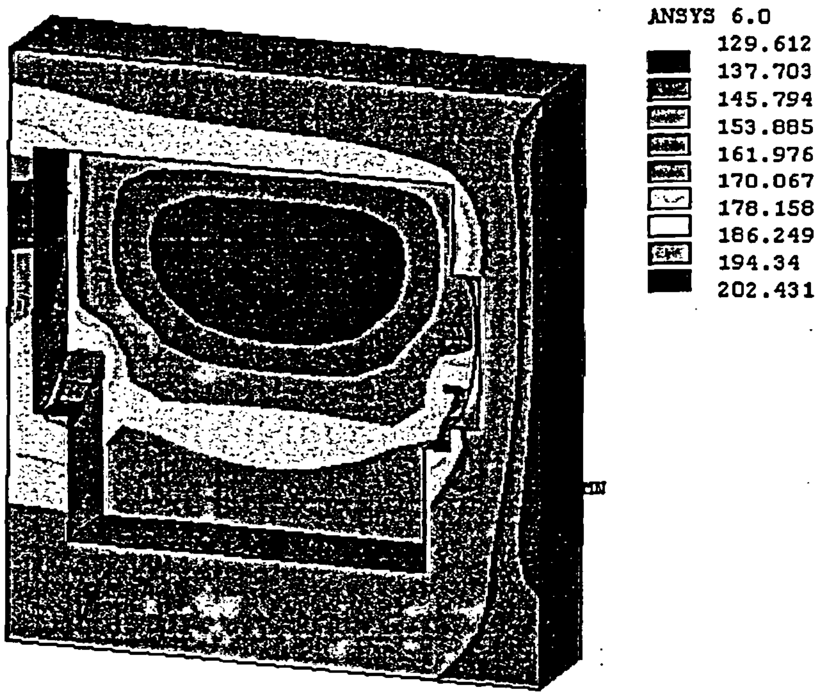

Figure 17 – Temperature Distribution – 40.8kW, 100°F Ambient

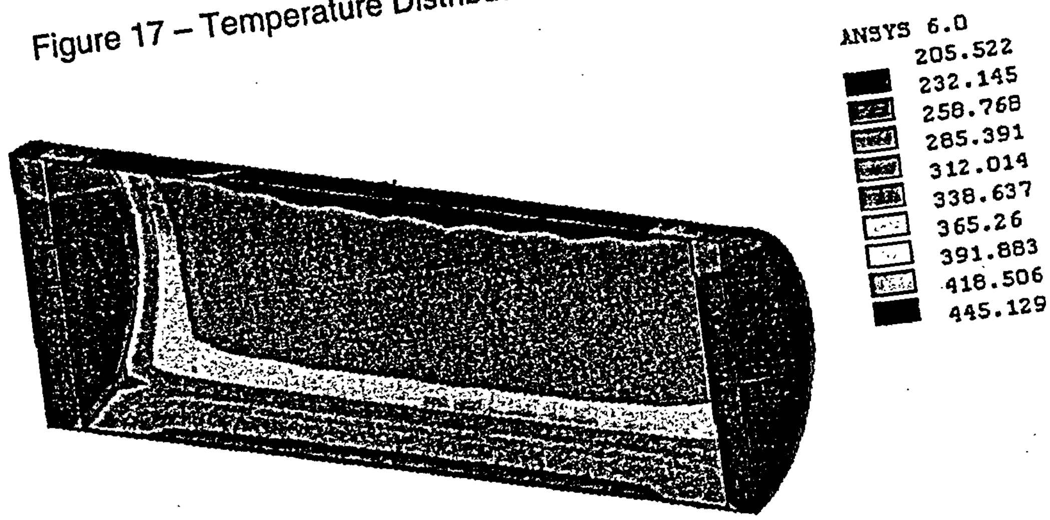

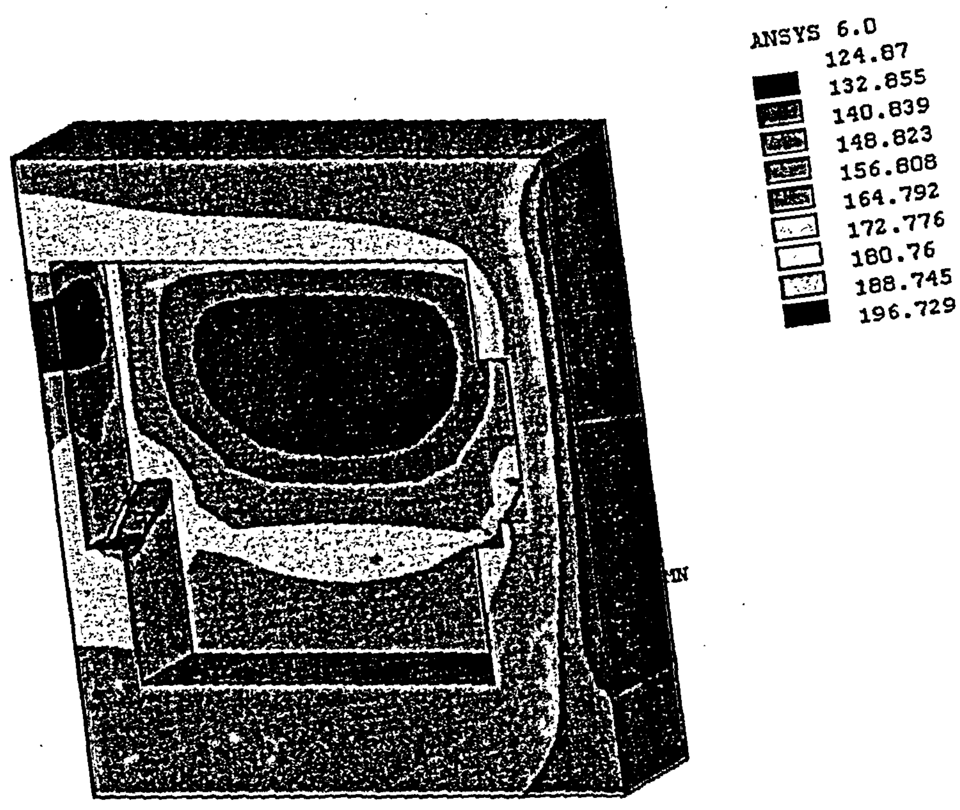

Figure 18 – Temperature Distribution – 40.8kW, 0°F Ambient

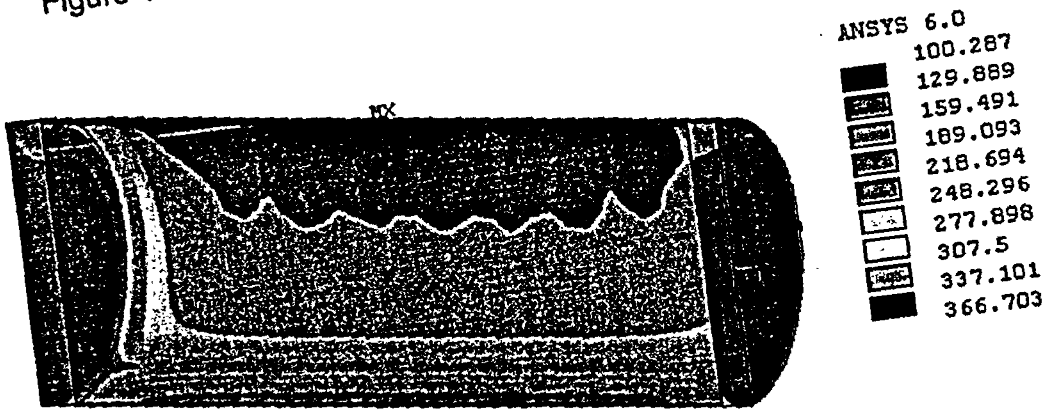

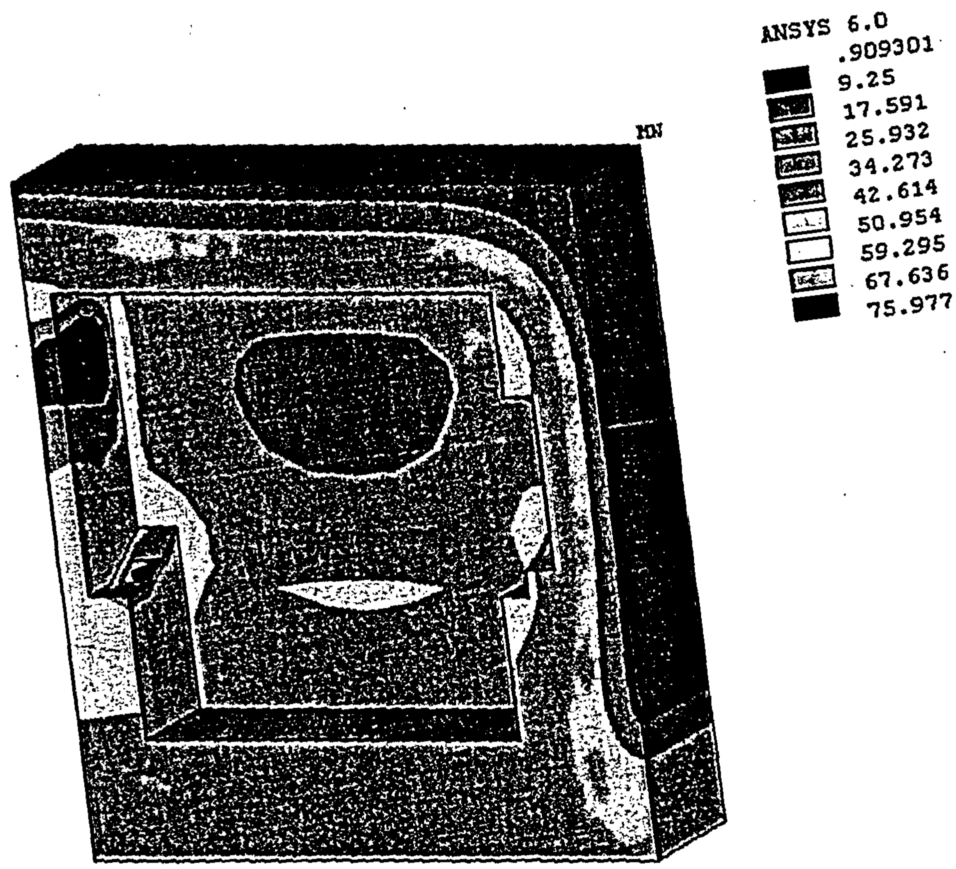

Figure 19 – Temperature Distribution – 40.8kW, -40°F Ambient

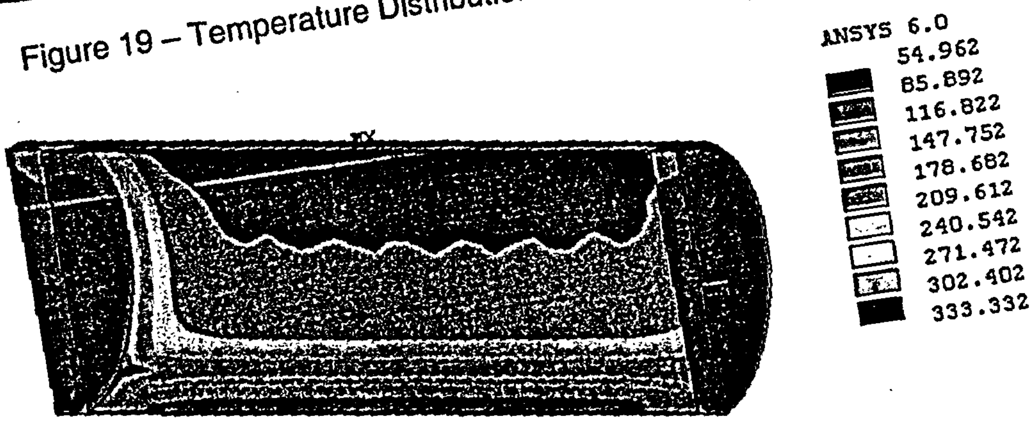

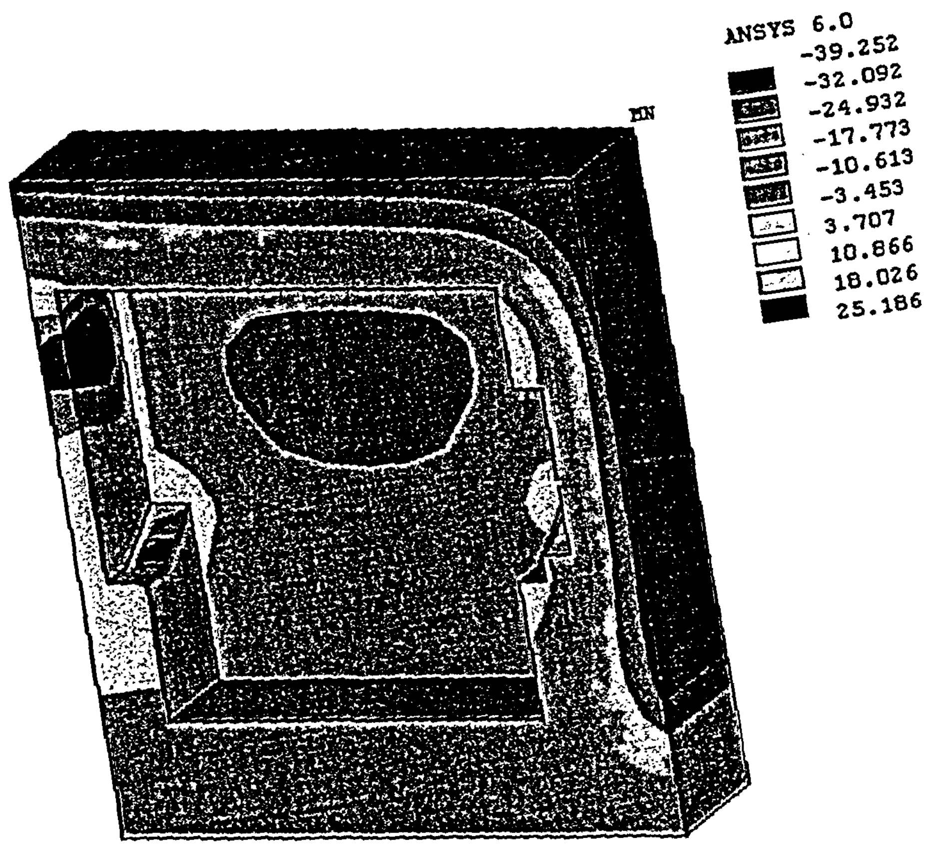

Figure 20 – Temperature Distribution – Blocked Vents for 38.5 hours 40.8 kW, 117°F Ambient

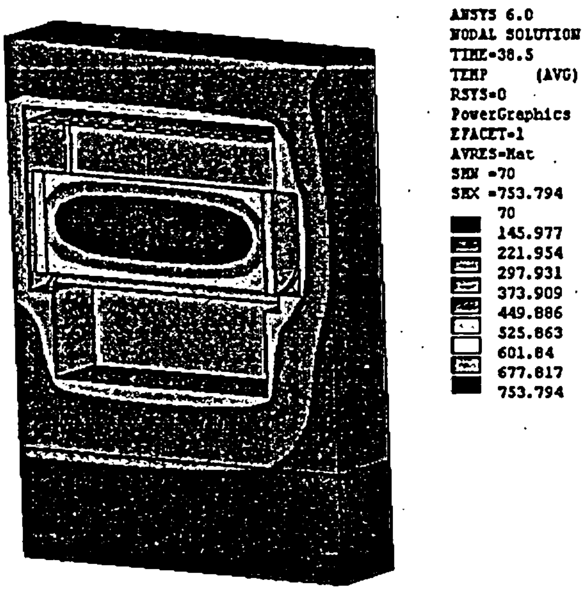

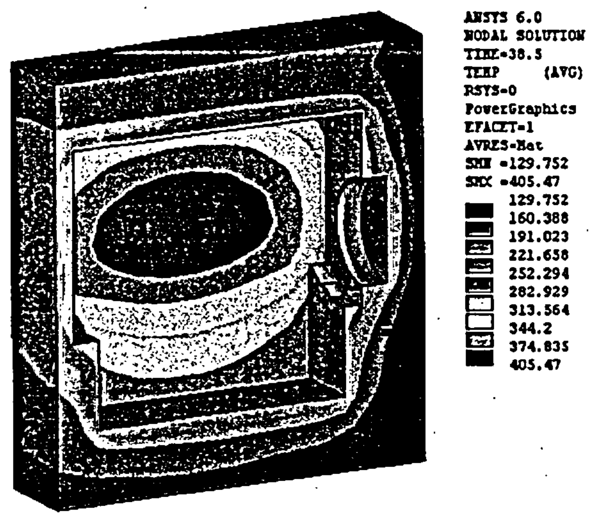

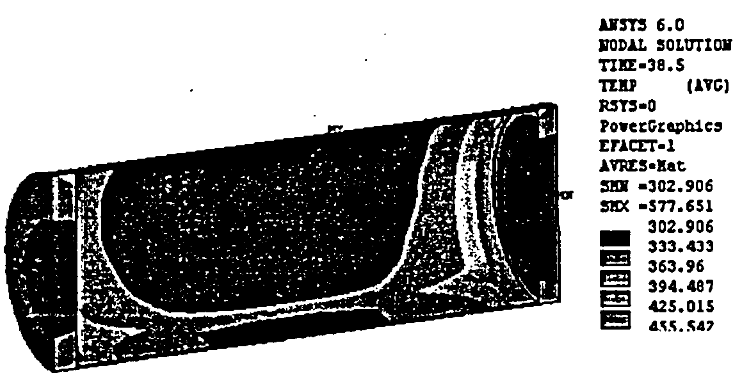

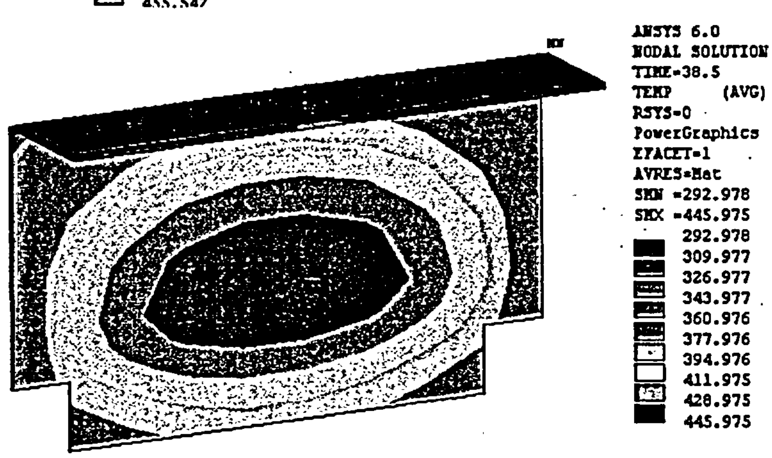

Figure 21 – Temperature-Time History of the Maximum Temperatures for the Blocked Vents Accident Case, 40.8 kW, 117°F Ambient

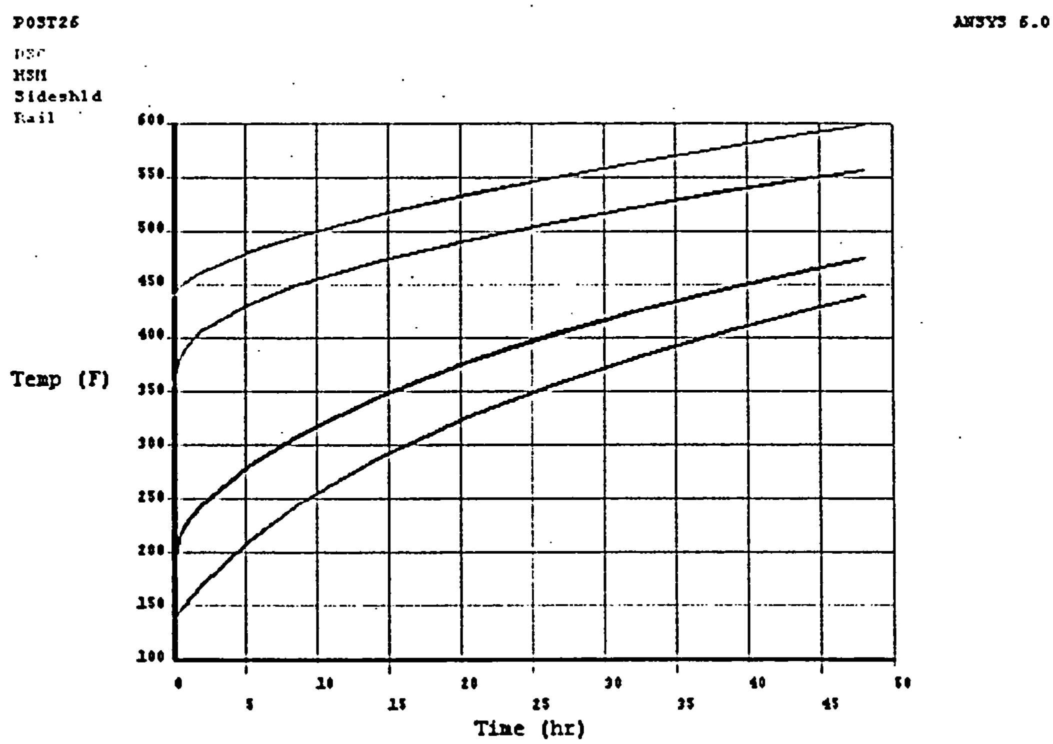

TRANSNUCLEAR, INC.

TITLE NUHOMS-24PTH, Thermal Analysis of the HSM Storage Conditions	SHEET 41 OF 59
	CALC. NO 60977-03
	REV. 0

Figure 22 – Temperature Distribution – Single HSM-H, Maximum Temperature Gradients Through Concrete Walls – 40.8 kW, -40°F Ambient, Steady-State

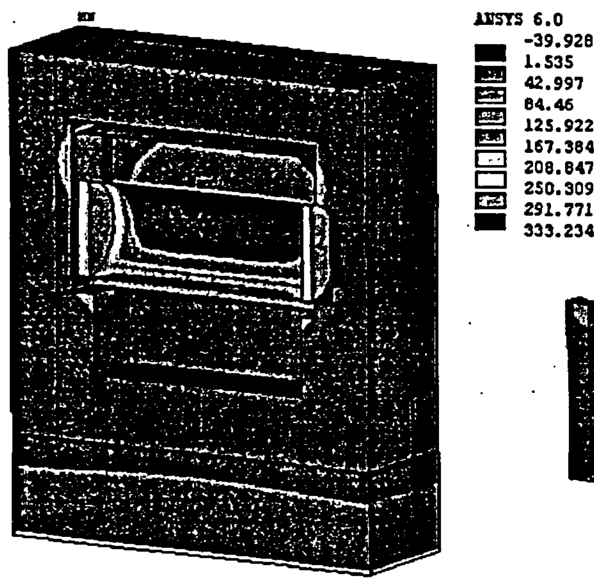

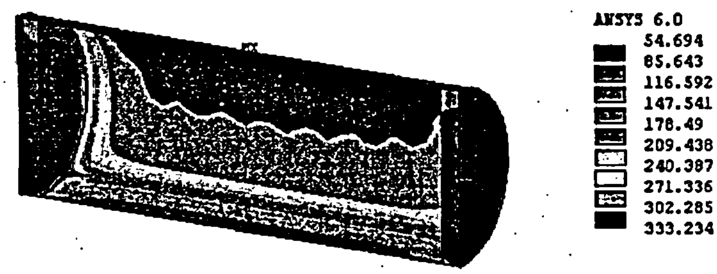

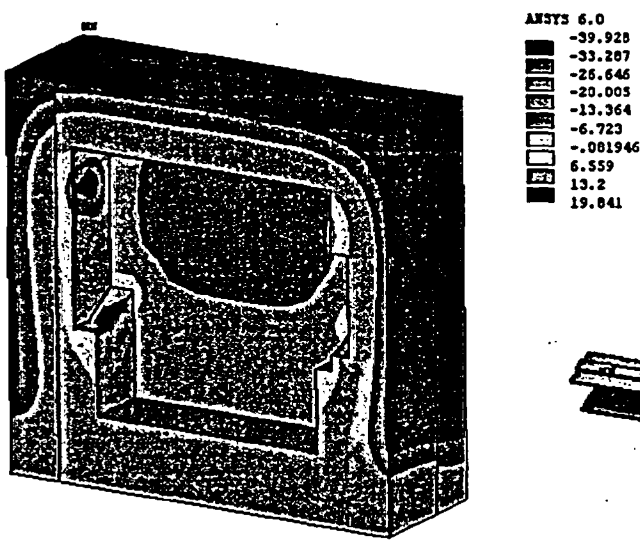

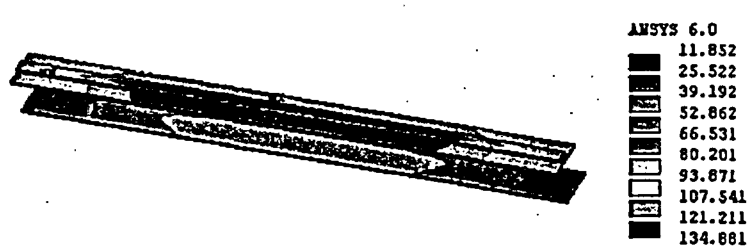

Figure 23 – Temperature Distribution – Single HSM-H, Blocked Vent for 38.5 hours
40.8 kW, -40°F Ambient, Transient

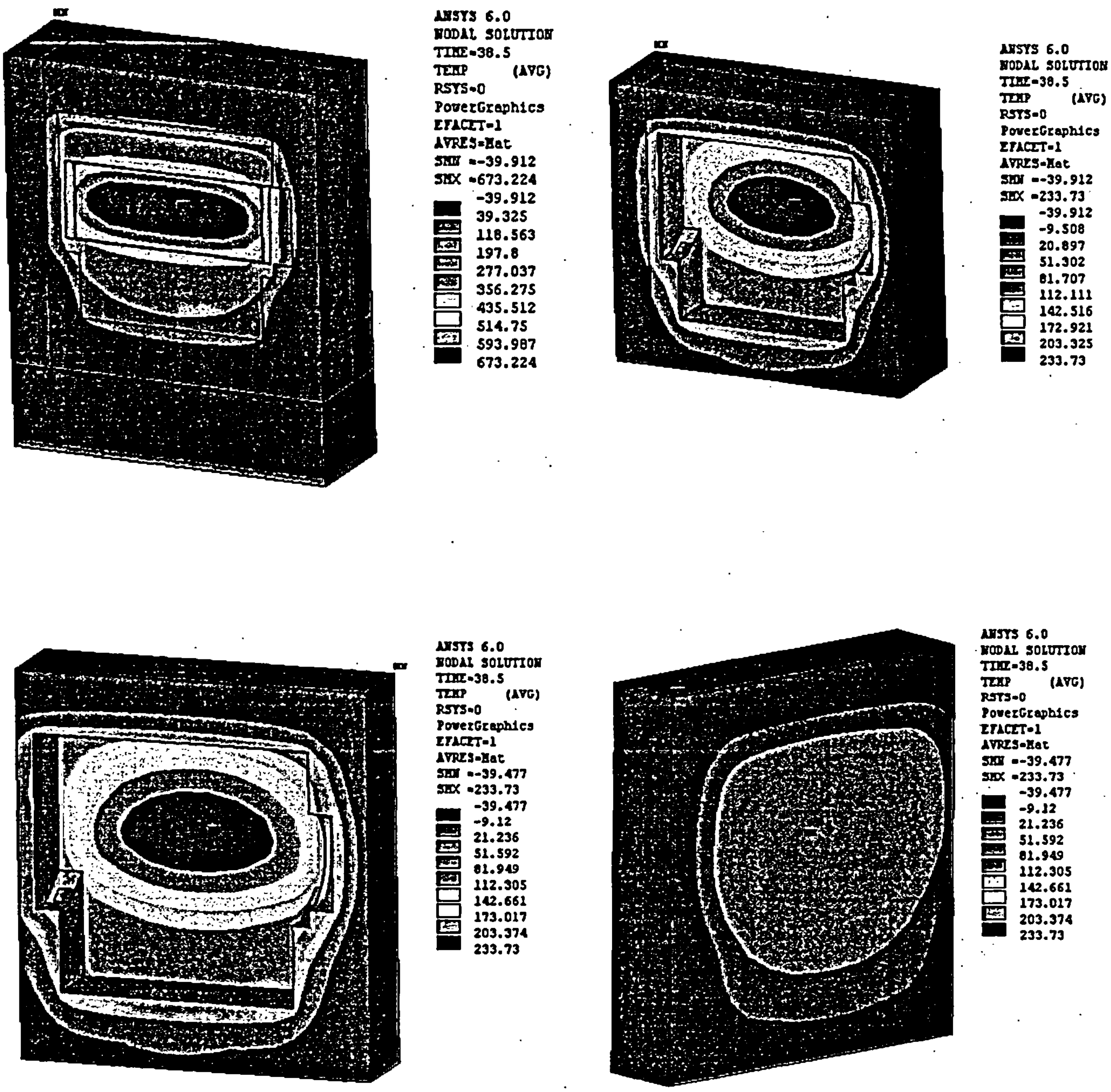

Appendix A

Convection Coefficient on Side Heat Shield

Figure A-1 shows the cross section of the side heat shield. Since the fin width, W, is much larger than the distance between the parallel fin plates, S, the convection coefficient is the same as for parallel –plate channel. Reference [14] specifies the following correlations for parallel-plate channels, when W/S≥5.

W=2.5", S=0.5" [2]

$$Nu \approx \frac{Ra}{24} \qquad \text{for } Ra \le 10$$

$$Nu = 0.62\ Ra^{1/4} \qquad \text{for } 10 < Ra < 1000$$

$$Nu = \left[\left(\frac{Ra}{24}\right)^m + \left(0.62 Ra^{1/4}\right)^m\right]^{1/m} \qquad \text{with } m=-1.9 \text{ for } Ra < 10^5$$

Rayleigh number for the above correlations is defined in Figure A-2.

Since the average plate temperature is first unknown, the model is solved iteratively. The final results are:

Case #	1	2	3	4	5	6	7	8
Conditions	24 kW, -40°F	24 kW, 117°F	31.2 kW, -40°F	31.2 kW, 117°F	40.8kW, -40°F	40.8kW, 0°F	40.8kW, 100°F	40.8kW, 117°F

Case	T_w ††	T_{amb} ‡‡	T_{avg}	T_{avg}	k [14]	β	ν [14]	Pr [14]	C_l	Ra	Nu	h_fin
#	(°F)	(°F)	(°F)	(K)	(W/m-K)	(1/K)	(m^2/s)	---	---	---	---	(Btu/hr-in^2-°F)
1	140	129	135	330	0.029	3.03E-03	1.91E-05	0.70	0.514	17.9	1.3	0.0035
2	-13	-23	-18	246	0.022	4.07E-03	1.14E-05	0.73	0.516	63.4	1.7	0.0037
3	157	134	146	336	0.029	2.97E-03	1.97E-05	0.70	0.514	34.4	1.5	0.0042
4	-5	-19	-12	249	0.022	4.02E-03	1.17E-05	0.72	0.516	83.3	1.9	0.0040
5	172	140	156	342	0.029	2.92E-03	2.04E-05	0.70	0.514	44.2	1.6	0.0045
6	166	134	150	339	0.029	2.95E-03	2.00E-05	0.70	0.514	46.3	1.6	0.0045
7	52	28	40	278	0.024	3.60E-03	1.41E-05	0.72	0.515	87.0	1.9	0.0045
8	6	-15	-5	253	0.022	3.95E-03	1.20E-05	0.72	0.516	115.7	2.0	0.0044

†† Average air temperature within the HSM-H, T_s [3]

‡‡ Average side heat shield temperature retrieved from model results [21]

The fins are modeled as a flat plat to reduce the number of SHELL57 elements in creation of radiation super-element. To compensate for the reduced area, an effective convection coefficient is calculated for the fins.

$$h_{fin,eff} = h_{fin} \cdot \frac{A_{fins}}{A_{model}}$$

$$A_{fin} = \left(2\, n_{up} \times 4 + 2 n_{down}\right) H\, W$$

number of fins at upper half: $n_{up} = (15'2"-4")/(0.5"+0.125")+1 = 285$ [2]

number of fins at lower half: $n_{down} = (15'2"-44")/(0.5"+0.125")+1 = 221$ [2]

H= 20" [2]

W = 2.5" [2]

$A_{fin} = 136100$ in^2

$A_{model} = [15'2"\times 7'2"+1'10"\times(15'2"-2\times 1'8")] = 18776$ in^2

$$h_{fin,eff} = 0.0044 \cdot \frac{136100}{18776} = 0.03$$ Btu/hr-in-°F highest value for hot conditions

$$h_{fin,eff} = 0.0035 \cdot \frac{136100}{18776} = 0.03$$ Btu/hr-in-°F lowest value for cold conditions

The value of h_{fin} used in the model is 0.031 Btu/hr-in-°F for hot and cold conditions.

Distance between the base plate of the side heat shield and the HSM-H side wall is 2" [2]. The base plate and the HSM-H side wall build up a narrow channel behind the side heat shield. The convection coefficient for this narrow channel is calculated using the same methodology described above. The dimensions of the narrow channel behind the side heat shield used to calculate the convection coefficient are:

S = 2"
H = 108"
W = 182"

The above dimensions are taken from [2]. The final surface temperature of the narrow channel is verified after iterative solution of the model. The final results are:

Case #	1	2	3	4	5	6	7	8
Conditions	24 kW, -40°F	24 kW, 117°F	31.2 kW, -40°F	31.2 kW, 117°F	40.8kW, -40°F	40.8kW, 0°F	40.8kW, 100°F	40.8kW, 117°F

Case	T_w §§	T_{amb} ***	T_{avg}	T_{avg}	k [14]	β	ν [14]	Pr [14]	C_l	Ra	Nu	h_channel
#	(°F)	(°F)	(°F)	(K)	(W/m-K)	(1/K)	(m^2/s)	---	---	---	---	(Btu/hr-in^2-°F)
1	140	108	124	324	0.028	3.08E-03	1.849E-05	0.70	0.514	2690	4.5	0.003
2	-21	-38	-30	239	0.021	4.18E-03	1.087E-05	0.73	0.516	5785	5.4	0.003
3	148	109	129	327	0.028	3.06E-03	1.875E-05	0.70	0.514	3161	4.6	0.003
4	-15	-37	-26	241	0.021	4.15E-03	1.104E-05	0.73	0.516	7204	5.7	0.003
5	160	110	135	331	0.029	3.03E-03	1.913E-05	0.70	0.514	3849	4.9	0.003
6	154	105	130	328	0.028	3.05E-03	1.881E-05	0.70	0.514	3940	4.9	0.003
7	38	4	21	267	0.024	3.74E-03	1.321E-05	0.72	0.515	6936	5.7	0.003
8	-7	-36	-22	244	0.022	4.11E-03	1.124E-05	0.73	0.516	9045	6.0	0.003

The value of $h_{channel}$ used in the model is 0.003 Btu/hr-in-°F for hot and cold conditions.

Air properties for calculation of convection coefficients are taken from [14] and listed in Table A-1.

Table A-1 – Air Properties [14]

Temperature	v	Conductivity	Prandtl	Dyn. Visc.
(K)	(m3/kg)	(W/m-K)	(-----)	(Pa-s)
200	0.573	0.0181	0.740	1.33E-05
300	0.861	0.0263	0.708	1.85E-05
400	1.148	0.0336	0.694	2.30E-05
500	1.436	0.0404	0.688	2.70E-05
600	1.723	0.0466	0.690	3.06E-05
800	2.298	0.0577	0.705	3.70E-05
1000	2.872	0.0681	0.707	4.24E-05

Temperature	ρ	Conductivity	Prandtl	Kin. Visc.
(F)	(lbm/ft^3)	(Btu/hr-ft-F)	(-----)	(ft^2/hr)
-100	0.109	0.0105	0.740	0.2953
80	0.073	0.0152	0.708	0.6172
260	0.054	0.0194	0.694	1.0232
440	0.043	0.0233	0.688	1.5024
620	0.036	0.0269	0.690	2.0430
980	0.027	0.0333	0.705	3.2948
1340	0.022	0.0393	0.707	4.7187

§§ Temperasure of air entering into channel, T_0 [3]

*** Average nodal temperature of narrow channel, retrieved from model results [21]

Figure A-1 – Side Shield Cross Section

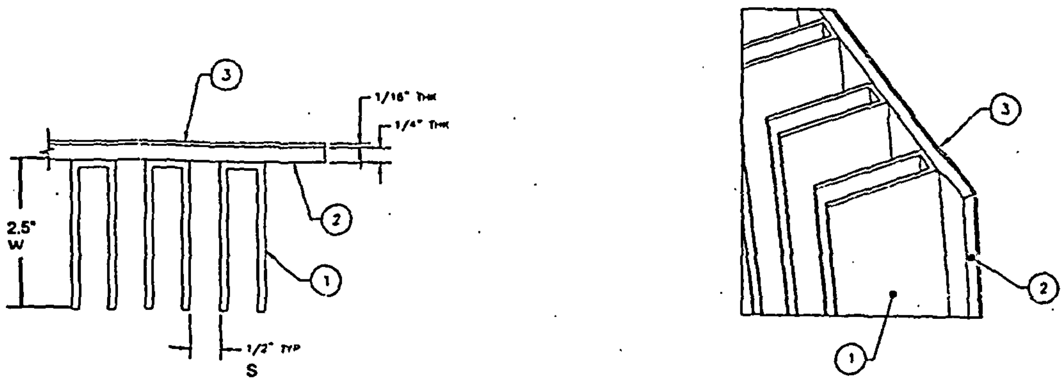

ITEM NO	QTY REQD	PART OR IDENTIFYING NO	NOMENCLATURE OR DESCRIPTION	MATERIAL SPECIFICATION	QUALITY CATEGORY
5	14		MOUNTING BAR	--	--
4	A/R		TOP HEAT SHIELD FINS, 1/8" THK	--	--
3	3		BACKING PLATE	ALUMINUM	--
2	3		BASE PLATE	ANODIZED ALUMINUM	--
1	A/R		HEAT SHIELD FINS	ANODIZED ALUMINUM	--

PARTS LIST

Figure A-2 – Convection Coefficient for Parallel-Plate Channels [14]

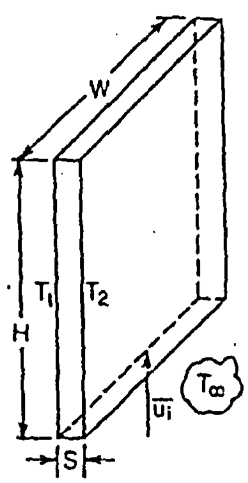

Specified wall temperatures

$$Nu = \frac{qS}{2HW(\overline{T}_w - T_\infty)k}$$

$$Ra = \frac{g\beta(\overline{T}_w - T_\infty)S^3}{\nu\alpha} \frac{S}{H}$$

$$Re = \overline{u_i}\, S/\nu$$

$$\overline{T}_w = \frac{1}{2}(T_1 + T_2)$$

$$T^* = \frac{T_2 - T_\infty}{T_1 - T_\infty};\ T_1 \geq T_2;\ 0 \leq T^* \leq 1$$

Geometry and nomenclature for natural-convection heat transfer from a wide ($W \gg S$), rectangular cooling slot with temperature-specified conditions on the walls.

Appendix B

Heat Transfer Coefficients

The following equations from Reference [14] are used to calculate the free convection coefficients.

For horizontal cylinders (DSC):

$$Ra = Gr \Pr \quad ; \quad Gr = \frac{g\beta(T_w - T_\infty)D^3}{\nu^2}$$

$$Nu_l = \frac{2f}{\ln(1+2f/Nu^T)}$$ Nusselt number for fully laminar heat transfer with

$$Nu^T = 0.772\,\overline{C}_l\,Ra^{1/4} \quad , \quad f = 1 - \frac{0.13}{(Nu^T)^{0.16}},$$ and $\overline{C}_l = 0.515$ for gases [14]

$$Nu_t = \overline{C}_t\,Ra^{1/3}$$ Nusselt number for fully turbulent heat transfer

$\overline{C}_t = 0.103$ for horizontal cylinders [15]

$$Nu = \left[(Nu_l)^m + (Nu_t)^m\right]^{1/m} \quad with \quad m = 3.3 \quad for \quad 10^{-10} < Ra < 10^{10}$$

$$h_c = \frac{Nu\,k}{D}$$ with

D = diameter of the horizontal cylinder
k = air conductivity

The above correlations are incorporated in ANSYS model via macro "HC_HCL.mac".

For vertical flat surfaces (end wall, side wall, vertical surface of the DSC plugs, and side heat shield without fins):

$$Ra = Gr \Pr \quad ; \quad Gr = \frac{g\beta(T_w - T_\infty)L^3}{\nu^2}$$

$$Nu_l = \frac{2.8}{\ln(1+2.8/Nu^T)}$$ Nusselt number for fully laminar heat transfer with

$$Nu^T = \overline{C}_l\,Ra^{1/4} \quad , \quad \overline{C}_l = 0.515$$ for gases [5]

$$Nu_t = C_t^V\,Ra^{1/3}$$ Nusselt number for fully turbulent heat transfer with

$$C_t^V = \frac{0.13\Pr^{0.22}}{(1+0.61\Pr^{0.81})^{0.42}}$$

$$Nu = \left[(Nu_l)^m + (Nu_t)^m\right]^{1/m} \quad with \quad m = 6 \quad for \quad 1 < Ra < 10^{12}$$

$$h_c = \frac{Nu\, k}{L}$$ with

L = height of the vertical surface

k = air conductivity

The above correlations are incorporated in ANSYS model via macro "HC_VPL.mac".

For horizontal surfaces facing upwards (basemat):

$$Ra = Gr\,\Pr \quad ; \quad Gr = \frac{g\,\beta(T_w - T_\infty)L^3}{\nu^2}$$

$$Nu_l = \frac{1.4}{\ln(1 + 1.4/Nu^T)}$$ Nusselt number for fully laminar heat transfer with

$Nu^T = 0.835\,\overline{C}_l\,Ra^{1/4}$, and $\overline{C}_l = 0.515$ for gases [14]

$Nu_t = C_t^H\,Ra^{1/3}$ Nusselt number for fully turbulent heat transfer

$C_t^H \approx 0.14$ for $\Pr < 100$ [14]

$$Nu = \left[(Nu_l)^m + (Nu_t)^m\right]^{1/m} \quad with \quad m = 10 \quad for \quad Ra > 1$$

$$h_c = \frac{Nu\, k}{L}$$ with

L = A/P

A=surface area of heated surface

P= perimeter of the heated surface

k = air conductivity

The above correlations are incorporated in ANSYS model via macro "HC_HPLU.mac".

For horizontal surfaces facing downwards (ceiling):

$$Ra = Gr\,\Pr \quad ; \quad Gr = \frac{g\,\beta(T_w - T_\infty)L^3}{\nu^2}$$

$$Nu_l = \frac{0.527\,Ra^{1/5}}{[1 + (1.9/\Pr)^{9/10}]^{2/9}}$$

$$Nu = Nu_l$$

$$h_c = \frac{Nu\, k}{L}$$ with

L = A/P
A=surface area of heated surface
P= perimeter of the heated surface
k = air conductivity

The above correlations are incorporated in ANSYS model via macro "HC_HPLD.mac".

For inclined surfaces, positive angled (web and upper side of supporting beam flange):

Reference [14] gives the following correlations for free convection over inclined flat, plates. The angle of inclined surface is measured from vertical line. The positive or negative sign of the angle is defined in Figure B-1.

$$Ra = Gr\,\Pr \quad ; \quad Gr = \frac{g\,\beta (T_w - T_\infty) L^3}{\nu^2} \cos\phi$$

$$Nu_l = \frac{2.8}{\ln(1+2.8/Nu^T)}$$ Nusselt number for fully laminar heat transfer with

$$Nu^T = \overline{C}_l\, Ra^{1/4} \quad , \quad \overline{C}_l = 0.515$$ for gases

$$Nu_t = C_t\, Ra^{1/3}$$ Nusselt number for fully turbulent heat transfer with

$$C_t = C_t^V \cos^{1/3}\phi \quad \text{for} \quad -90^\circ \le \phi \le \tan^{-1}\left(\frac{C_t^V}{C_t^H}\right)^3$$

$$C_t = C_t^H \sin^{1/3}\phi \quad \text{for} \quad \tan^{-1}\left(\frac{C_t^V}{C_t^H}\right)^3 \le \phi \le 90^\circ$$

with

$$C_t^V \approx \frac{0.13\Pr^{0.22}}{(1+0.61\Pr^{0.81})^{0.42}}$$

$$C_t^H \approx 0.14 \quad for \quad \Pr < 100$$

$$Nu = \left[(Nu_l)^m + (Nu_t)^m\right]^{1/m} \quad with \quad m = 6 \quad for \quad 1 < Ra < 10^{12}$$

$$h_c = \frac{Nu\,k}{L}$$ with

L = length of the inclined plate
k = air conductivity

The above correlations are incorporated in ANSYS model via macro "HC_IPLU.mac".

For inclined surfaces, negative angled (lower side of supporting beam flange):

$$Ra = Gr\,\Pr \quad ; \quad Gr = \frac{g\,\beta (T_w - T_\infty) L^3}{\nu^2} \times \cos\phi$$

$$Nu_{l,V} = \frac{2.8}{\ln(1 + 2.8 / Nu^T)}$$

$$Nu^T = \overline{C}_l\, Ra^{1/4} \qquad , \overline{C}_l = 0.515$$ for gases

$$Nu_{l,H} = \frac{0.527\, Ra^{1/5}}{[1 + (1.9/\Pr)^{9/10})^{2/9}}$$

$$Nu_l = \max[Nu_{l,V}, Nu_{l,H}]$$ Nusselt number for fully laminar heat transfer

$$Nu_t = C_t \; Ra^{1/3}$$ Nusselt number for fully turbulent heat transfer with

$$C_t = C_t^V \cos^{1/3}\phi \qquad \text{for} \qquad -90^\circ \le \phi \le \tan^{-1}\left(\frac{C_t^V}{C_t^H}\right)^3$$

$$C_t = C_t^H \sin^{1/3}\phi \qquad \text{for} \qquad \tan^{-1}\left(\frac{C_t^V}{C_t^H}\right)^3 \le \phi \le 90^\circ$$

with $C_t^V \approx \dfrac{0.13\Pr^{0.22}}{(1 + 0.61\Pr^{0.81})^{0.42}}$

$$C_t^H \approx 0.14 \qquad \textit{for} \qquad \Pr < 100$$

$$Nu = \left[(Nu_l)^m + (Nu_t)^m\right]^{1/m} \qquad \textit{with} \quad m = 6 \quad \textit{for} \;\; 1 < Ra < 10^{12}$$

$h_c = \dfrac{Nu\,k}{L}$ with

L = length of the inclined plate
k = air conductivity

The above correlations are incorporated in ANSYS model via macro "HC_IPLD.mac".

Convection Coefficient on Top Heat Shield

Top shield is a louver consists of seven pieces each containing 78 inclined plates. Figure B-2 shows the top heat shield. Because of the relative large opening between the plates and the short length of them, the interference of the thermal boundary layers is minimal,

so that convection coefficient can be calculated separately for each plate. The total convection from one inclined plate is:

$$q_{conv} = (h_{up} + h_{down}) A_p (T_p - T_\infty)$$

with h_{up} = convection coefficient on upper surface of louver plates (positive angled)
h_{down} = convection coefficient on lower surface of louver plates (negative angled)
plate surface $Ap = l \times h = 24 \times 2 = 48$ in^2 [2]
air temperature $T_\infty = T_8 = 178^\circ F$ [3]

h_{up} and h_{down} are calculated using the correlations described above for inclined plates. The louver is modeled as a flat plat to reduce the number of SHELL57 elements in creation of radiation super-element. To compensate for the reduced area, an effective convection coefficient is calculated for the louver.

$$h_{louver,eff} = (h_{up} + h_{down}) \cdot \frac{A_{louver}}{A_{model}}$$

$$A_{louver} = n_{louver} \times n_{segments} \times A_p$$

n_{louver} = no. of plates in each segment = 78 [2]
$n_{segments}$ = no. of segments = 7 [2]

$A_{model} = 15'2'' \times 6'2'' = 14196$ in^2 [2]

The above correlations are incorporated in ANSYS model via macro "HC_Louver.mac".

Total Heat Transfer Coefficient on Roof and Front Wall

The HSM roof and the front wall dissipate heat to the ambient via free convection and radiation. Total heat transfer coefficient, H_t, is used to combine the convection and radiation heat transfer together.

$$H_t = h_r + h_c$$

where,

h_r = radiation heat transfer coefficient
h_c = free convection heat transfer coefficient, horizontal surface facing upwards for roof and vertical, flat surface for front wall

The radiation heat transfer coefficient, h_r, is given by the equation:

$$h_r = \varepsilon F_{12}\left[\frac{\sigma(T_1^4 - T_2^4)}{T_1 - T_2}\right] Btu/hr - ft^2 \text{-}^\circ F$$

where,

ε = surface emissivity

F_{12} = view factor from surface 1 to ambient

σ = 0.1714×10^{-8} Btu/hr-ft^2-R^4

T_1 = surface temperature, R

T_2 = ambient temperature, R

The above correlations are incorporated in ANSYS model via macros "HC_ROOF.mac" and "HC_FRONT.mac".

Figure B-1 – Definition of Surface Angel ϕ for a Heated Wall [14]

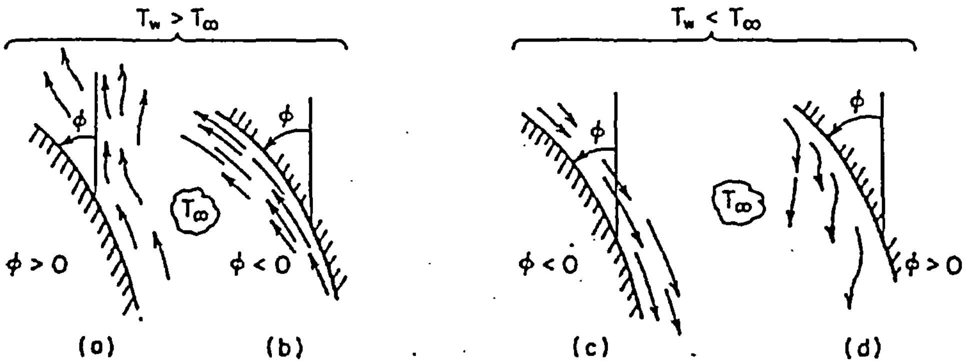

Definition of surface angle ϕ for a heated wall (*a* and *b*), and a cooled wall (*c* and *d*). If the flow is turbulent, *a* and *d* depict detached flow, *b* and *c* attached flow.

TRANSNUCLEAR, INC.

TITLE	NUHOMS-24PTH, Thermal Analysis of the HSM Storage Conditions	SHEET 54 OF 59	
		CALC. NO	60977-03
		REV.	0

Figure B-2 – Dimensions of the Top Heat Shield

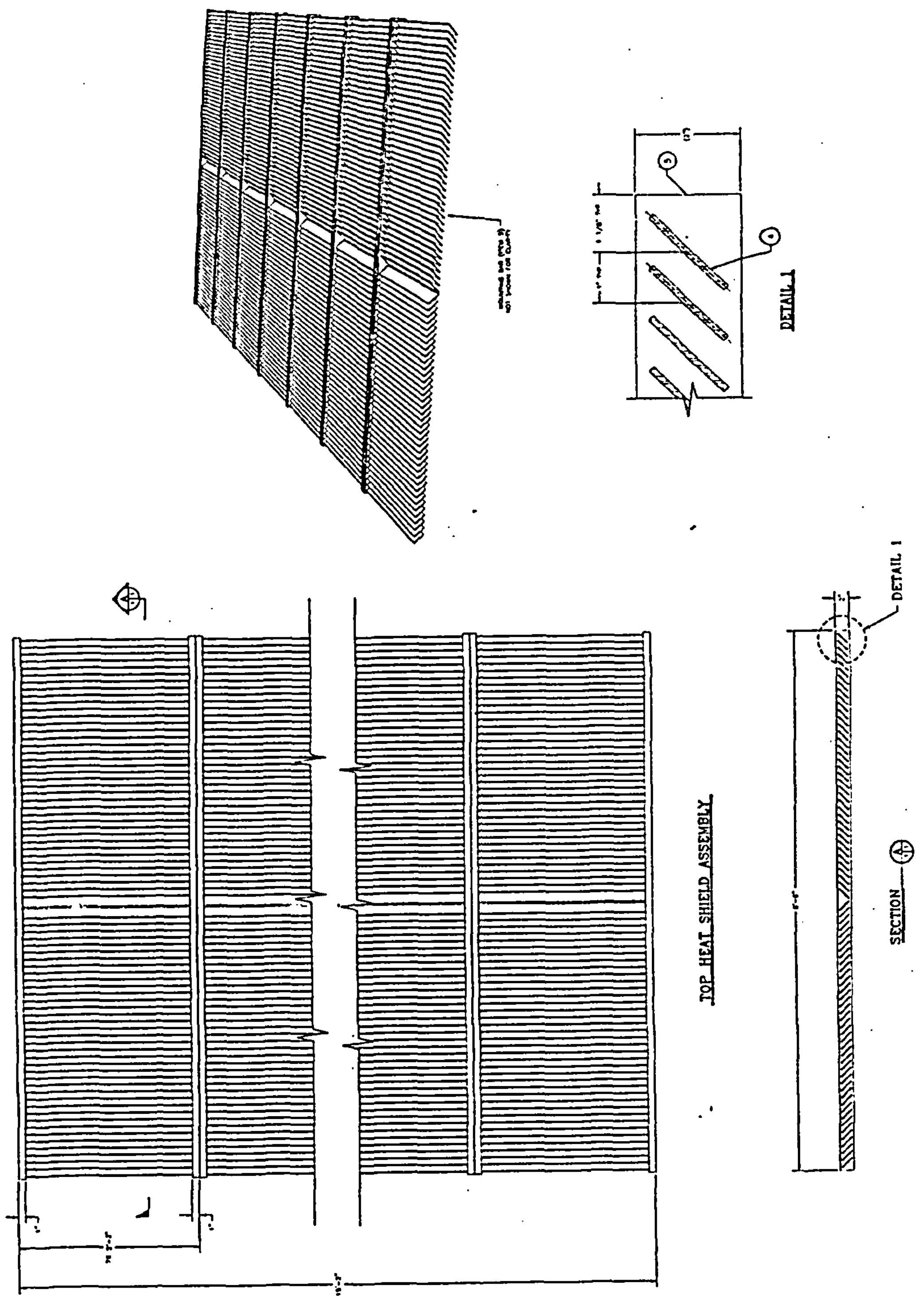

Appendix C

Effect of Non-Idealities on Temperature Distribution in the HSM-H Model

C.1 - Thermal Effects of the Support Structure Emissivity

A study is performed to investigate the sensitivity of the component temperatures to the emissivity value selected for the support structure. In the study the emissivity of support structure is reduced from 0.9 to 0.3 in the finite element model of the HSM-H. All the dimension, material properties, boundary conditions remain the same as those for the off-normal case with 105F daily average temperature (117°F maximum daylight temperature) and 40.8 kW decay heat load.

The resultant temperature distributions for support structure emissivity of 0.3 are shown in Figure C-1. The maximum component temperatures for emissivities of 0.3 and 0.9 are listed in the following table.

Table C-1 – Comparison of the Maximum Temperatures for Various Support Structure Emissivities

	40.8 kW, 117°F ambient, $\varepsilon = 0.3$	40.8 kW, 117°F ambient, $\varepsilon = 0.9$
Component	**Max. Temp. (°F)**	**Max. Temp. (°F)**
DSC Shell	449	448
Concrete	203	202
Top shield	188	188
Side Shield	182	181
Support Rail	297	280

As the above table shows all the maximum component temperatures are increased by less than 1°F except for the support structure. Reducing the emissivity of the support structure decreases the amount of the radiation heat transfer from the support structure to the surrounding surfaces and causes higher temperature in the support structure. The maximum temperature of the support structure might be considered conservatively at 297°F or higher for other calculations using the result of this analysis. The effect of decreasing the support structure emissivity is insignificant for the other HSM-H components.

C.2 - Thermal Effects of the Offset Sidewall and Higher Bulk Temperature

As discussed in section 3, the offset side wall is not considered in the HSM-H model for simplification. In addition, the air bulk temperatures calculated in the finalized version of [3]

are slightly higher than the values used in the HSM-H model. The bulk temperatures within the HSM-H are listed below for 40.8 kW and 117F ambient case.

Table C-2 – Air Temperatures in the HSM Cavity

	40.8 kW Decay Heat, 117°F Ambient	
Location	Temperature	Value (°F)
Lower part of HSM	T_0	110
DSC Region 1	T_1	115
DSC Region 2	T_2	125
DSC Region 3	T_3	135
DSC Region 4	T_4	145
DSC Region 5	T_5	155
DSC Region 6	T_6	165
DSC Region 7	T_7	175
DSC Region 8	T_8	185
Air Bulk Temp	T_s	141

The HSM-H model is modified to evaluate the effect of the above discrepancies on the temperature distribution within the HSM-H. The emissiviy of the support structure is set to 0.3 in the modified model. The modified model is shown in Figure C-2. The resultant temperatures are listed in the following table.

Table C-2 – Comparison of the Maximum Temperatures with and without Offset Sidewalls

	40.8 kW, 117°F ambient, offset wall, higher bulk temp., ε = 0.3	**40.8 kW, 117°F ambient, straight wall, lower bulk temp., ε = 0.9**
Component	**Max. Temp. (°F)**	**Max. Temp. (°F)**
DSC Shell	450	448
Concrete	204	202
Top shield	190	188
Side Shield	183	181
Support Rail	297	280

Figure C-3 shows the temperature distributions in the modified model. Similar to the first study, the maximum component temperatures are increased by about 2°F except for the support structure. The temperature increase of the support structure is caused by the lower emissivity applied on support structure as shown in the first study. The effect of the offset wall and slightly higher bulk temperatures affect the other HSM-H component temperatures insignificantly.

Figure C-1 – Temperature Distributions in the HSM-H with ε=0.3 for Support Structure

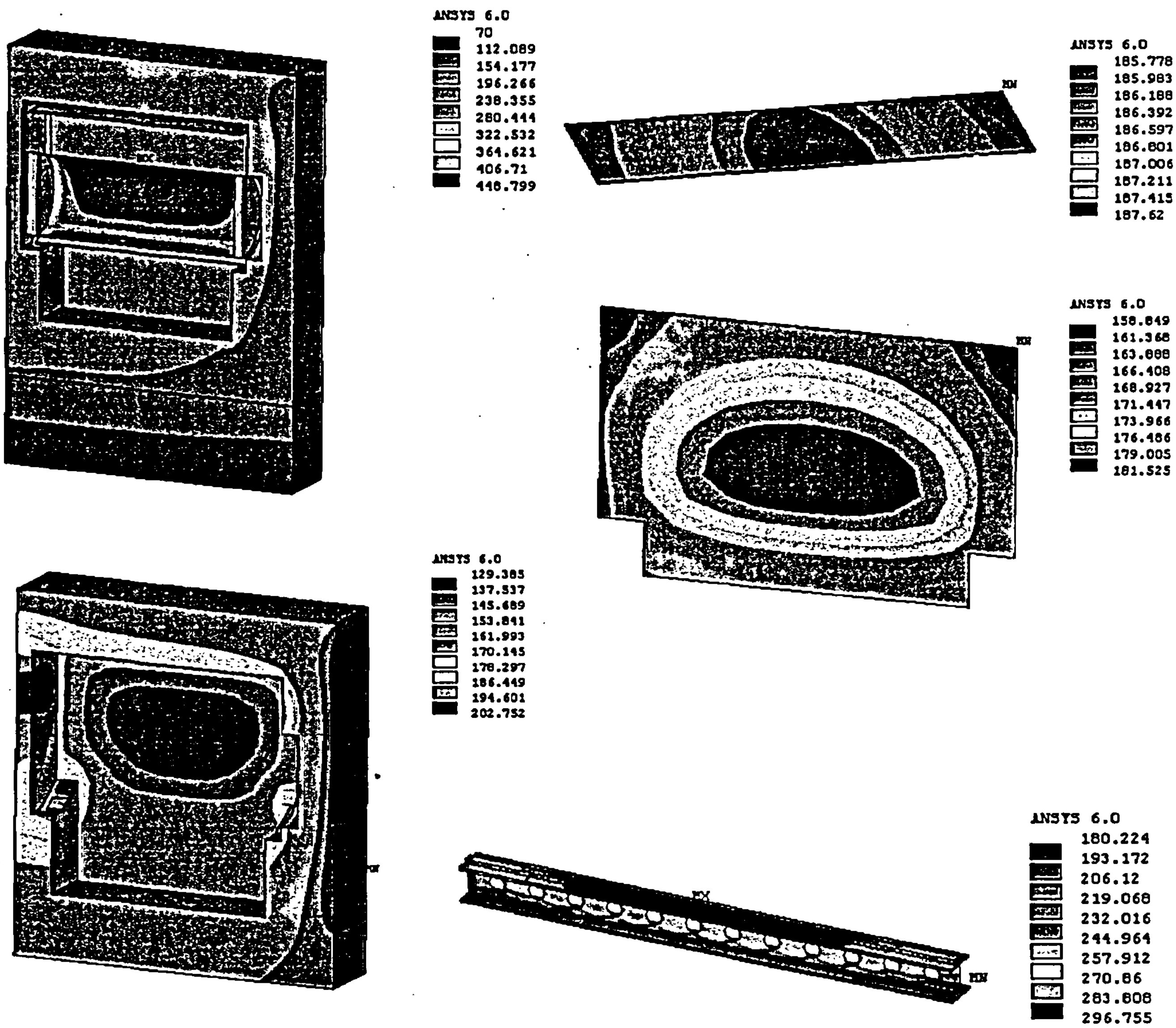

Figure C-2 – Finite Element Model with Offset Sidewall

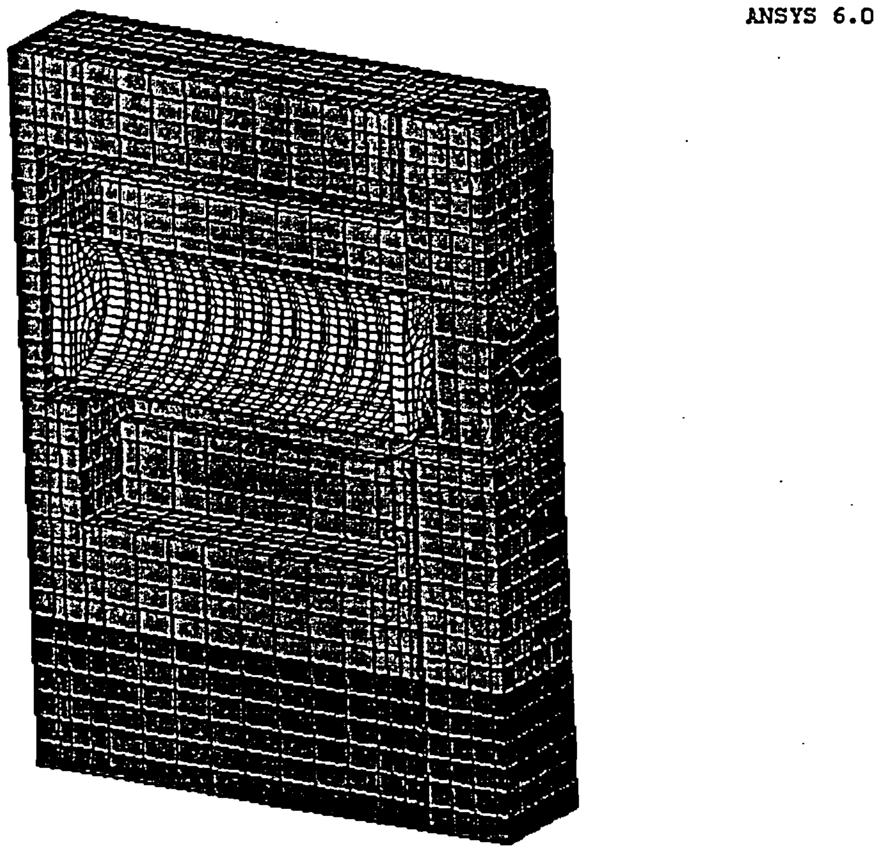

TRANSNUCLEAR, INC.

TITLE	NUHOMS-24PTH, Thermal Analysis of the HSM Storage Conditions	SHEET 59 OF 59	
		CALC. NO	60977-03
		REV.	0

Figure C-3 – Temperature Distributions in the HSM-H with Offset Sidewalls, Higher Bulk Temperatures, and ε=0.3 for Support Structure

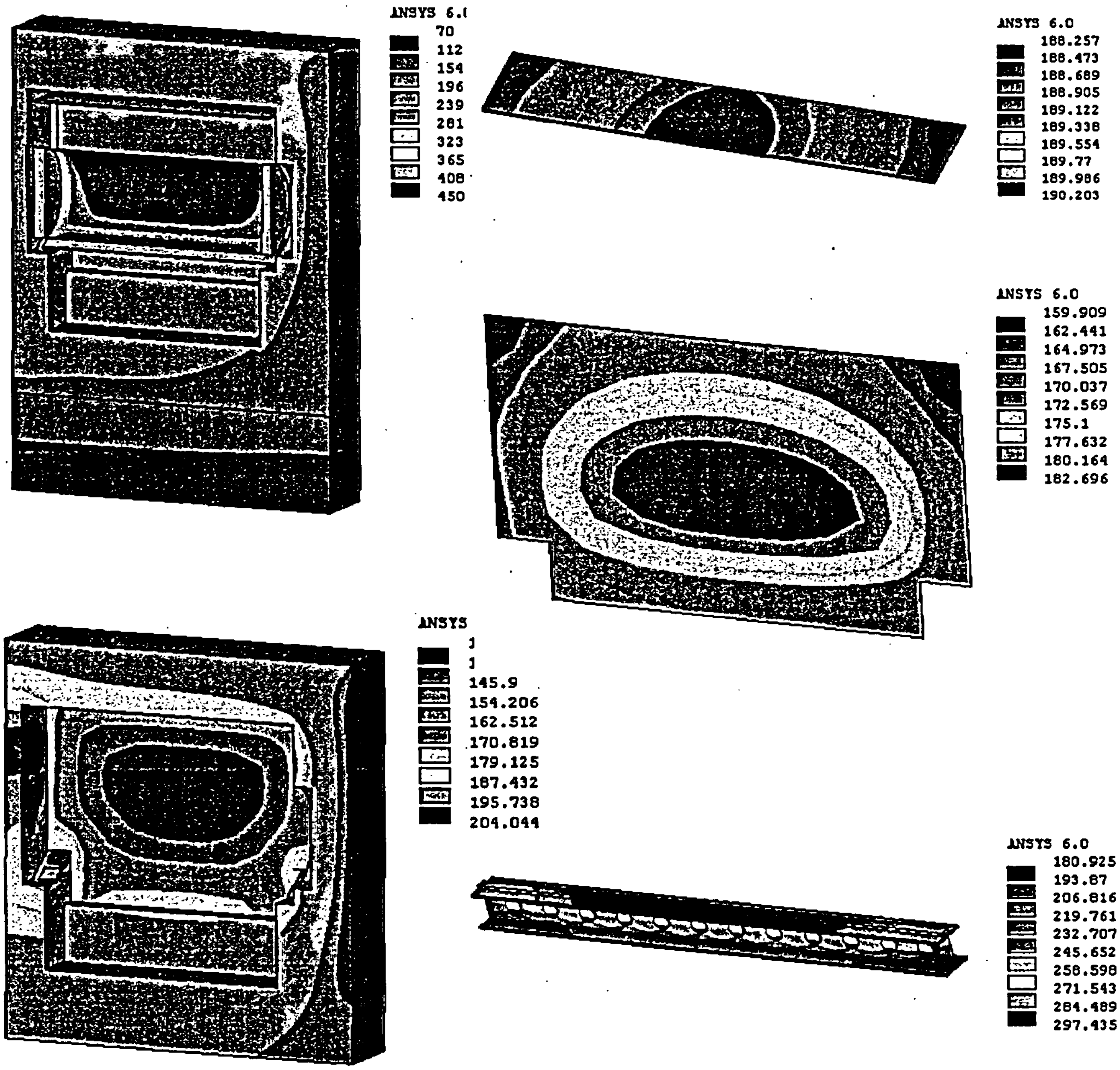

AFFIDAVIT PURSUANT TO 10 CFR 2.790

Transnuclear, Inc.	)	
State of Washington	)	SS.
County of Pierce	)	

I, William D. Gallo, depose and say that I am Senior Vice President of Transnuclear, Inc., duly authorized to make this affidavit, and have reviewed or caused to have reviewed the information which is identified as proprietary and referenced in the paragraph immediately below. I am submitting this affidavit in conformance with the provisions of 10 CFR 2.790 of the Commission's regulations for withholding this information.

The information for which proprietary treatment is sought is contained in the calculation packages included in Enclosure 2 of this submittal and as listed below:

- Calculation NUH24PTH.0420, Revision 1 (One Copy and One CD),
- Calculation NUH24PTH.0421, Revision 0 (One Copy and One CD), and
- Calculation NUH32PT.0414, Revision 0 (One Copy and One CD).

This section of the document and these input files have been appropriately designated as proprietary.

I have personal knowledge of the criteria and procedures utilized by Transnuclear, Inc. in designating information as a trade secret, privileged or as confidential commercial or financial information.

Pursuant to the provisions of paragraph (b) (4) of Section 2.790 of the Commission's regulations, the following is furnished for consideration by the Commission in determining whether the information sought to be withheld from public disclosure, included in the above referenced document, should be withheld.

1) The information sought to be withheld from public disclosure are specific Calculation packages relating to the analysis of the NUHOMS® Cask, which is owned and has been held in confidence by Transnuclear, Inc.

2) The information is of a type customarily held in confidence by Transnuclear, Inc. and not customarily disclosed to the public. Transnuclear, Inc. has a rational basis for determining the types of information customarily held in confidence by it.

3) The information is being transmitted to the Commission in confidence under the provisions of 10 CFR 2.790 with the understanding that it is to be received in confidence by the Commission.

4) The information, to the best of my knowledge and belief, is not available in public sources, and any disclosure to third parties has been made pursuant to regulatory provisions or proprietary agreements which provide for maintenance of the information in confidence.

5) Public disclosure of the information is likely to cause substantial harm to the competitive position of Transnuclear, Inc. because:

a) A similar product is manufactured and sold by competitors of Transnuclear, Inc.

b) Development of this information by Transnuclear, Inc. required considerable of man-hours and resources. To the best of my knowledge and belief, a competitor would have to undergo similar expense in generating equivalent information.

c) In order to acquire such information, a competitor would also require considerable time and inconvenience related to the development of a design and analysis of a dry spent fuel storage system.

d) The information required significant effort and expense to obtain the licensing approvals necessary for application of the information. Avoidance of this expense would decrease a competitor's cost in applying the information and marketing the product to which the information is applicable.

e) The information consists of description of the design and analysis of a dry spent fuel storage and transportation system, the application of which provides a competitive economic advantage. The availability of such information to competitors would enable them to modify their product to better compete with Transnuclear, Inc., take marketing or other actions to improve their product's position or impair the position of Transnuclear, Inc.'s product, and avoid developing similar data and analyses in support of their processes, methods or apparatus.

f) In pricing Transnuclear, Inc.'s products and services, significant research, development, engineering, analytical, licensing, quality assurance and other costs and expenses must be included. The ability of Transnuclear, Inc.'s competitors to utilize such information without similar expenditure of resources may enable them to sell at prices reflecting significantly lower costs.

Further the deponent sayeth not.

William D. Gallo
Senior Vice President, Transnuclear, Inc.

Subscribed and sworn to me before this 21st day of January, 2004, by William D. Gallo.

Bonnie M Hargis
Notary Public

BONNIE M. HARGIS
COMMISSION EXPIRES
NOTARY
PUBLIC
10-14-03
STATE OF WASHINGTON